



LJMU Research Online

Sharwood, RE, Ghannoum, O, Kapralov, MV, Gunn, LH and Whitney, SM

Temperature responses of Rubisco from Paniceae grasses provide opportunities for improving C3 photosynthesis.

<http://researchonline.ljmu.ac.uk/id/eprint/5501/>

Article

Citation (please note it is advisable to refer to the publisher's version if you intend to cite from this work)

Sharwood, RE, Ghannoum, O, Kapralov, MV, Gunn, LH and Whitney, SM (2016) Temperature responses of Rubisco from Paniceae grasses provide opportunities for improving C3 photosynthesis. Nature Plants, 2. ISSN 2055-0278

LJMU has developed **LJMU Research Online** for users to access the research output of the University more effectively. Copyright © and Moral Rights for the papers on this site are retained by the individual authors and/or other copyright owners. Users may download and/or print one copy of any article(s) in LJMU Research Online to facilitate their private study or for non-commercial research. You may not engage in further distribution of the material or use it for any profit-making activities or any commercial gain.

The version presented here may differ from the published version or from the version of the record. Please see the repository URL above for details on accessing the published version and note that access may require a subscription.

For more information please contact researchonline@ljmu.ac.uk

<http://researchonline.ljmu.ac.uk/>

1 **Variation in response of C₃ and C₄ Paniceae Rubisco to temperature**
2 **provides opportunities for improving C₃ photosynthesis**

3

4 Robert E. Sharwood¹⁺, Oula Ghannoum^{2+*}, Maxim V. Kapralov³, Laura H. Gunn^{1,4}, and
5 Spencer M. Whitney^{1+*}.

6

7 ¹Research School of Biology, Australian National University, Canberra ACT, 2601,
8 Australia.

9 ²Hawkesbury Institute for the Environment, Western Sydney University, Richmond,
10 New South Wales, 2753, Australia.

11 ⁺ ARC Centre of Excellence for Translational Photosynthesis, Australian National
12 University Canberra ACT, 2601, Australia.

13 ³Current Address: School of Natural Sciences and Psychology, Liverpool John Moores
14 University, Liverpool, L3 3AF, United Kingdom

15 ⁴Current address: Department of Cell and Molecular Biology, Uppsala University,
16 Uppsala, SE-751 24, Sweden.

17 *Corresponding Authors: o.ghannoum@westernsydney.edu.au and
18 spencer.whitney@anu.edu.au

19 **Abstract:**

20 Enhancing the catalytic properties of the CO₂-fixing enzyme Rubisco is a target for
21 improving agricultural crop productivity. Here we reveal high diversity in the kinetic
22 response between 10°C to 37°C by Rubisco from C₃- and C₄-species within the grass tribe
23 Paniceae. The CO₂-fixation rate (k_{cat}^C) for Rubisco from the C₄-grasses with NADP-malic
24 enzyme (NADP-ME) and phosphoenolpyruvate carboxykinase (PCK) photosynthetic
25 pathways was two-fold greater than the k_{cat}^C of Rubisco from NAD-ME species over all
26 temperatures. The decline in the response of CO₂/O₂ specificity with increasing
27 temperature was slower for PCK and NADP-ME Rubisco – a trait which would be
28 advantageous in the warmer climates they inhabit relative to the NAD-ME grasses.
29 Variation in the temperatures kinetics of Paniceae C₃-Rubisco and PCK-Rubisco were
30 modelled to differentially stimulate C₃-photosynthesis above and below 25°C under current
31 and elevated CO₂. Identified are large subunit amino acid substitutions that could account
32 for the catalytic variation among Paniceae Rubisco. Incompatibilities with Paniceae
33 Rubisco biogenesis in tobacco however hindered their mutagenic testing by chloroplast
34 transformation. Circumventing these bioengineering limitations is critical to tailoring the
35 properties of crop Rubisco to suit future climates.

36 Concerns about how escalating climate change will influence ecosystems are particularly
37 focused on the consequences to global agricultural productivity where increases are
38 paramount to meet the rising food and biofuel demands. Strategies to improve crop yield
39 by increasing photosynthesis have largely focused on overcoming the functional
40 inadequacies of the CO₂-fixing enzyme Rubisco. A competing O₂-fixing reaction by
41 Rubisco produces a toxic product whose recycling by photorespiration consumes energy
42 and releases carbon. The frequency of the oxygenation reaction increases with temperature.
43 To evade photorespiration many plants from hot, arid ecosystems have evolved C₄
44 photosynthesis that concentrates CO₂ around Rubisco that also facilitates improved plant
45 water, light and nitrogen use. Here we show extensive catalytic variation in Rubisco from
46 Paniceae grasses that align with the biochemistry and environmental origins of the different
47 C₄ plant subtypes. We reveal opportunities for enhancing crop photosynthesis under
48 current and future CO₂ levels at varied temperatures.

49 The realization of the dire need to address global food security has heightened the need for
50 new solutions to increase crop yields¹. Field tests and modelling analyses have highlighted
51 how photosynthetic carbon assimilation underpins the maximal yield potential of crops².
52 This has increased efforts to identify solutions to enhance photosynthetic efficiency and
53 hence plant productivity³. Particular attention is being paid to improving the rate at which
54 ribulose-1,5-bisphosphate carboxylase/oxygenase (Rubisco, EC 4.1.1.39) can fix CO₂
55 (refs 4–8). The complex structure and catalytic chemistry of Rubisco has so far made
56 improving its performance difficult^{9–11}. Diversity screens have identified natural Rubisco
57 variants with catalytic improvements of potential benefit^{11–17}, but most overlook the
58 influence of broad changes in temperature.

59 In C₃-plants Rubisco performance is hampered by slow CO₂-fixation rates (k_{cat}^C
60 ~2-3 s⁻¹) and competitive O₂-fixation that produces 2-phosphoglycolate, which requires
61 recycling by the energy-consuming and CO₂-releasing photorespiratory cycle. This
62 necessitates C₃-plants invest up to 50% of their leaf protein (~25% of their nitrogen) into
63 Rubisco to sustain viable CO₂ assimilation rates¹⁻³. A reduction in the atmospheric CO₂:O₂
64 ratio during the Oligocene period (~30 million years ago) heightened plant photorespiration
65 rates, particularly in hot, arid environments⁴. This led to the convergent evolution of C₄
66 photosynthesis along >65 multiple independent plant lineages⁵. C₄-plants contain a CO₂
67 concentrating mechanism (CCM) that allows Rubisco in the chloroplasts of bundle sheath
68 cells (BSC) to operate under near-saturating CO₂ levels. This suppresses O₂-fixation and
69 photorespiration. The BSC CCM begins in the adjoining mesophyll cells (MC) where
70 inorganic carbon, as HCO₃⁻, is fixed to phosphoenolpyruvate (PEP) by PEP carboxylase
71 (PEPC) to form the C₄-acid oxaloacetate (OAA). Conversion of OAA to malate (or
72 aspartate) precedes its diffusion into the BSC where it is decarboxylated to elevate CO₂
73 around Rubisco. The three biochemical subtypes of C₄-plants correlate to the dominant
74 decarboxylation enzyme: nicotinamide adenine dinucleotide (NAD) phosphate malic
75 enzyme (NADP-ME), NAD malic enzyme (NAD-ME) or phosphoenolpyruvate
76 carboxykinase (PEP-CK)^{6,7}.

77 An escalating appreciation of the significant kinetic variation among plant, algae
78 and prokaryotic Form I Rubisco has, until recently, paid little consideration to the
79 functional diversity and potential of C₄-Rubisco to improve C₃-photosynthesis⁸.
80 Adaptation of C₄-Rubisco to elevated BSC CO₂ has beneficially increased carboxylation
81 rate (k_{cat}^C) but unfavourably lowered CO₂-affinity (*i.e.* increased K_m for CO₂). The increase

82 in k_{cat}^C endows C₄-plants with accompanying improvements in their nitrogen (less Rubisco
83 required), water (reduced stomata apertures needed) and energy (reduced photorespiration)
84 use efficiencies⁹ – features considered of potential benefit to engineering in C₃-plants¹⁰.
85 What remains unclear is the extent to which variation in the ancestral timing, CCM
86 biochemistry and biogeographical origin has influenced the kinetic evolution C₄-Rubisco,
87 its response to temperature and it's potential to benefit C₃-photosynthesis without a CCM.

88 Here we examine the diversity in the temperature response (10°C to 37°C) of
89 Rubisco catalysis in Paniceae grasses comprising species with C₃, C₃-C₄ intermediate (C₂)
90 and all three C₄ biochemical subtypes. We identify significant variation in the kinetic
91 properties of Paniceae Rubisco which correlates with the photosynthetic physiology and
92 environmental distribution of each species. We show by modelling how the potential of
93 Paniceae Rubisco to differentially improve C₃-photosynthesis at low and high temperatures
94 under current and future CO₂. Differences in the chaperone requirements of monocot
95 Rubiscos are revealed that prevent use of chloroplast transformation to validate Paniceae
96 Rubisco “catalytic switches” using the surrogate model dicot plant tobacco.

97 **Materials and Methods**

98 **Plant Seeds and Growth Conditions**

99 Seeds for *Panicum antidotale*, *P. monticola*, *P. virgatum*, *P. milliaceum*, *P. coloratum*, *P.*
100 *deustum*, *P. milioides*, *P. bisulcatum*, *Megathyrsus maximus*, *Urochloa panicoides*, *U.*
101 *mosambicensis*, *Cenchrus ciliaris*, *Setaria viridis* and *Steinchisma laxa* were obtained
102 from Australian Plant Genetic Resources Information System (QLD, Australia) and
103 Queensland Agricultural Seeds Pty. Ltd., (Toowoomba, Australia) (Table S1) and sown in
104 germination trays containing a common germination mix. Three to four weeks after
105 germination, three seedlings were transplanted into 5L pots containing potting mix and
106 grown in the glass house under natural illumination at 28°C/22°C D/N. Plants were watered
107 regularly with the addition of a commercial of liquid fertilizer (General Purpose, Thrive
108 Professional, Yates, Australia).

109 **Leaf dry matter carbon isotope composition**

110 Leaf dry matter carbon isotope composition was determined to confirm which species use
111 the C₄ photosynthetic pathway. Leaf discs were oven-dried then combusted in a Carlo Erba
112 elemental analyser (Model 1108, Milan, Italy). The emitted CO₂ was analyzed by mass
113 spectrometry (VG Isotech, Manchester, UK) and the $\delta^{13}\text{C}$ was calculated as $[(R_{\text{sample}} -$
114 $R_{\text{standard}}) / R_{\text{standard}}] * 1000$, where R_{sample} and R_{standard} are the ¹³C/¹²C ratio of the sample and
115 the standard Pee Dee Belemnite (PDB), respectively

116 **Rubisco catalytic measurements**

117 Rates of ¹⁴CO₂ fixation by fully activated Rubisco were measure at 10 to 37°C using
118 soluble leaf protein extracted from 0.5 to 2.0 cm² of leaf material extracted in 1 mL

119 extraction buffer as described by Sharwood et al (2008)¹¹. Preliminary assays as described
120 in Sharwood et al., (2016)¹² were used to confirm the suitability of the extraction process
121 for sustained maximal activity over 30 min at 25°C. The ¹⁴CO₂ fixation assays (0.5 mL)
122 were performed in 7-mL septum-capped scintillation vials in reaction buffer (50 mM
123 EPPES-NaOH (pH 8.19 at 25°C), 10 mM MgCl₂, 0.4 mM RuBP) containing varying
124 concentrations of NaH¹⁴CO₃ (0–40 μM) and O₂ (0–30%) (vol/vol), accurately mixed with
125 nitrogen using Wostoff gas-mixing pumps. The vials were incubated at the appropriate
126 assay temperature for at least 1 hr before adding 20 μL of the soluble leaf protein to initiate
127 the reaction. The assays were terminated with 0.1 mL of 20% (v/v) formic acid after 1 min
128 (for the assays at 25 to 37°C) or 2 min (for the assays at 10 to 20°C). The Rubisco kinetic
129 measurements were performed using two to six biological samples (see Table S2 for
130 detail). Each protein sample was assayed in duplicate following incubation at 25°C for 8
131 and 12 min. The carboxylation activity varied by <2% between each technical replicate.
132 This confirmed each Rubisco was fully activated after incubating 8 min at 25°C with no
133 detectable loss of activity after incubating a further 4 min. The Rubisco content
134 (determined by ¹⁴C-CABP binding¹²) and integrity of the extracted L₈S₈ holoenzyme
135 Rubisco was confirmed by non-denaturing PAGE¹³. For each experiment a soluble leaf
136 protein preparation was added to four assays containing the highest [¹⁴CO₂] and 5 nmol of
137 purified RuBP. After reacting to completion (1 to 3 h at different temperatures) they were
138 treated with formic acid, dried and processing for scintillation counting. The measured ¹⁴C
139 cpm in each assay varied by <0.5% and the average value divided by 5 to derive the ¹⁴CO₂
140 specific activity. The values for pH, pK₁, pK₂ and *q* (the CO₂ solubility at 1 atm) used to
141 calculate CO₂ levels in the assays at the different temperatures are provide in Table S5.

142 The Michaelis-Menton constants (K_m) for O_2 (K_O), for CO_2 under nitrogen (K_C) or air levels
143 of O_2 ($K_C^{21\%O_2}$) were determined from the fitted data. The maximal rate of carboxylation
144 (V_c^{max}) was extrapolated from the fitted data and the caboxylation rate (k_{cat}^c) derived by
145 dividing V_c^{max} by the Rubisco-catalytic site content quantified by [^{14}C]-2-CABP binding
146 ¹¹.

147 Rubisco CO_2/O_2 specificity ($S_{C/O}$) was measured using Rubisco rapidly purified by ion
148 exchange then Superdex 200 (GE Life Sciences) size exclusion column chromatography
149 ¹³. The assays were equilibrated with 500 ppm CO_2 mixed with O_2 using Wostoff gas-
150 mixing pumps and $S_{C/O}$ calculated using $CO_2:O_2$ solubility ratios of 0.033, 0.035, 0.036,
151 0.038, 0.039 and 0.041 at assay temperatures of 10, 15, 20, 25, 30 and 35°C, respectively
152 (see Table S5 for gas solubility detail).

153 ***rbcL* amplification, sequencing and phylogenetic alignment**

154 Replica genomic DNA preparations (2 to 4) from each grass species were purified from
155 ~0.5 cm² leaf discs using a DNeasy Plant Mini Kit (Qiagen) according to manufacturer's
156 instructions. The full length *rbcL* coding sequence (including adjoining 5'UTR and 3'UTR
157 sequence) was PCR amplified from each DNA preparation using primers 5'Pan*rbcL* (5'-
158 CTAATCCATATCGAGTAGAC -3') and 3'Pan*rbcL*DNA (5'-
159 AGAATTACTGCATTTTCGTAAC -3'). The amplified products varied in size between
160 species (1504 to 1589-bp) but each showed identical sequence for the independent DNA
161 preparations from each species. DNA sequences were translated into protein sequences and
162 aligned using MUSCLE (Edgar, 2004) and the *rbcL* phylogeny reconstructed using
163 maximum-likelihood inference conducted with RAxML version 7.2.6.

164 **Chloroplast transformation of *Panicum rbcL* into tobacco**

165 Plasmids pLevPdL and pLevPbL were biolistically transformed into the plastome of the
166 tobacco genotype ^{cm}trL1 as described ¹³ to derive the transplastomic genotypes tob^{PdL} and
167 tob^{PbL} that, respectively, coded the *rbcL* genes from *P. deustum* and *P. bisulcatum* (in
168 addition to the *aadA* gene coding spectinomycin resistance) in place of the tobacco *rbcL*
169 gene. RNA blot, [¹⁴C]-2-CABP binding and PAGE analyses of Rubisco expression were
170 performed on independent homoplasmic lines for each genotype as described above with
171 additional experimental detail provided in Figure S7.

172 **Statistical analysis**

173 Statistical analysis was carried out using one-way (species or photosynthetic type/ subtype)
174 or two-way analysis of variance, ANOVA (Statistica, StatSoft Inc. OK, USA). Means were
175 grouped using a Post-hoc Tukey test. Detailed description of the temperature response
176 analysis and modelling are provided in the Figure and Table legends for convenience.

177 **Results**

178 Our comprehensive evaluation of Rubisco kinetics within the Paniceae tribe included two
179 C₃, one C₃-C₄ intermediate (signified C₂⁷), four NADP-ME, four PCK and three NAD-ME
180 species (Table S1). Rubisco from tobacco, our model plant for Rubisco engineering and
181 that commonly used in biochemical modeling, was included as a control. The C₃ and C₄
182 physiologies of each species were confirmed using dry matter carbon isotope ratio ($\delta^{13}\text{C}$)
183 measurements (Table S1). As expected, the $\delta^{13}\text{C}$ kinetic isotope effect was significantly
184 lower in the C₂ and C₃ species ($\approx -28.7\text{‰}$) relative to the C₄ specie (≈ -13.3 to -14.6‰)
185 (Fig 1a).

186 **The carboxylation properties of Paniceae Rubisco synchronize with C₄-subtype.**

187 Substantial variation was found in the Rubisco kinetics measured at 25°C among enzymes
188 from C₂/C₃-species and each C₄-subtype (Table S1). Relative to the carboxylation rates
189 ($k_{\text{cat}}^{\text{c}}$) of the C₂/C₃ species, the Rubisco $k_{\text{cat}}^{\text{c}}$ was marginally higher in NAD-ME and 2-fold
190 greater in the NADP-ME and PCK species (Fig. 1b). Consistent with the co-dependency
191 of K_{C} and $k_{\text{cat}}^{\text{c}}$ ¹⁴, greater reductions in CO₂-affinity (*i.e.* higher K_{C} 's) were found for
192 Rubisco from NADP-ME and PCK species relative to the NAD-ME and C₂/C₃ species (Fig
193 1c). Less variation was observed for the averaged oxygenation rates ($k_{\text{cat}}^{\text{o}}$; Fig. 1d) and O₂-
194 affinities (K_{O} ; Fig. 1d) among C₃ and C₄ Rubisco. Nevertheless, the NADP-ME Rubiscos
195 tended to show less sensitivity to O₂ inhibition (*i.e.* a higher K_{O}). This improvement did
196 not, however, improve the specificity for CO₂ over O₂ ($S_{\text{C/O}}$) of NADP-ME Rubisco, which
197 was significantly lower than the more similar $S_{\text{C/O}}$ of Rubisco from the C₃, NAD-ME and
198 PCK species (Fig 1f).

199 Analysis of these core catalytic parameters underscored how the strong positive
200 correlation between $k_{\text{cat}}^{\text{c}}$ and K_{C} shared by plant Rubisco¹⁴⁻²¹ extends to Paniceae C₃- and
201 C₄-Rubisco (Fig 1g). Uniquely, each C₄-subtype Rubisco aggregated at a distinctive
202 position along the regression indicative of adaptation to the differences in CCM
203 efficiencies and biogeography among C₄-subtypes²², or reflective of differences in resource
204 partitioning to Rubisco that, in NADP-ME plants for example, correlate with improved N-
205 use efficiency⁹. The “subtype-grouping” of the carboxylase kinetics was not evident in the
206 increasingly weaker linear correlations between $k_{\text{cat}}^{\text{o}}$ and K_{O} (Fig 1h), $k_{\text{cat}}^{\text{c}}$ and $k_{\text{cat}}^{\text{o}}$ (Fig 1i)
207 and K_{C} with K_{O} (Fig 1j). Evidently, the coordinated changes in $k_{\text{cat}}^{\text{c}}$ and K_{C} for each
208 Paniceae C₄-subtype are not tightly coupled to changes in oxygenase kinetics. This feature

209 is common to Rubisco due to differences in the mechanism and energy profiles of the
210 carboxylation and oxygenation reactions, a property that has facilitated the evolution of
211 diverse Rubisco kinetics^{14,23}.

212 **The potential for Paniceae Rubisco to improve C₃-photosynthesis at 25°C.**

213 A recent study of Rubisco kinetic diversity revealed how the enzyme from some C₄-
214 species, such as the increased S_{C/O} and carboxylation efficiency under ambient O₂ ($k_{\text{cat}}^c /$
215 $K_C^{21\%O_2}$) of *Zea mays* (maize) NADP-ME Rubisco, has the potential to improve C₃-
216 photosynthesis⁸. The bi-functionality of Rubisco necessitates consideration of both O₂ and
217 CO₂-fixing activities when evaluating improvement within C₃-photosynthesis^{1,24,25}, and
218 does not necessarily accord with a higher $k_{\text{cat}}^{c1,8}$. A correlative analysis of these parameters
219 for Paniceae Rubisco identified a weak relationship between k_{cat}^c and S_{C/O} ($r^2 = 0.43$; Fig
220 2a) supporting mounting evidence that the trade-off proposed between these parameters^{14,21}
221 shows significant natural divergence^{18,26}. Differences in O₂ inhibition among the Paniceae
222 Rubisco (*i.e.* variable K_O values, Fig 1e) resulted in $K_C^{21\%O_2}$ values (quantified as
223 $K_C(1+[O_2]/K_O)$) that showed a weaker co-dependence with k_{cat}^c ($r^2 = 0.76$; Fig 2b) relative
224 to K_C ($r^2 = 0.88$; Fig 1g). This underscores the inaccuracy of using K_C measures as a proxy
225 to interpret the relative CO₂-affinity of Rubisco under ambient O₂ (*i.e.* $K_C^{21\%O_2}$).

226 The biochemical models of Farquhar et. al., (1980)²⁴ provide a useful tool to
227 evaluate how the kinetic properties of Rubisco influence carbon assimilation in C₃-plants.
228 These C₃-models often use tobacco Rubisco as the reference^{1,8,27,28}. This stems from
229 tobacco having well characterized Rubisco kinetics, it being the model species for
230 bioengineering Rubisco by chloroplast and nucleus transformation, and its potential to
231 support higher rates of photosynthesis at 25°C under low chloroplast CO₂ pressures (C_c)

232 than wheat Rubisco^{8,29}. Figure 2c shows comparable C₃-modeling using the averaged S_{C/O},
233 $k_{\text{cat}}^c / K_C^{21\%O_2}$ and k_{cat}^c values from each Paniceae biochemical subtype (Table S1). Under
234 low C_c where CO₂-assimilation rates are carboxylase limited, Rubisco from the NADP-
235 ME and PCK species would support higher rates of photosynthesis than the Paniceae C₃
236 and NAD-ME and tobacco Rubisco (Fig 2c). Under higher C_c where photosynthesis
237 becomes limited by light dependent rates of electron transport the lower S_{C/O} of the
238 Paniceae C₄-Rubiscos would support lower rates of CO₂-assimilation relative to tobacco.
239 In contrast the higher S_{C/O} of Paniceae C₃-Rubisco would enhance their CO₂-assimilating
240 capacity at C_c's above ~240 μbar (Fig 2c).

241 **The temperature diversity of Paniceae Rubisco**

242 Most diversity screens of Rubisco kinetics are undertaken at 25°C and possibly one or two
243 other temperatures^{18,20,30,31}. More rigorous studies providing kinetics that can be
244 extrapolated over a broad temperature range have primarily focused on Rubisco from C₃-
245 plants^{15,19,28,32,33}. In general, the level of kinetic variation has been sufficient to highlight
246 weakness in the customary use of the temperature response for tobacco Rubisco kinetics²⁷
247 to reliably model the photosynthetic responses of other species. This weakness is
248 particularly apparent from our high precision temperature response measurements that
249 reveal substantial kinetic diversity among Paniceae Rubisco from NAD-ME, NADP-ME,
250 PCK and C₂/C₃ groupings (Fig 3). The parameters analyzed were S_{C/O}, k_{cat}^c and $K_C^{21\%O_2}$
251 (averting the need to measure K_O for C₃-modeling purposes) at six incremental
252 temperatures between 10 and 37°C (Fig S1 to S3). The activation energies (ΔH_a) for each
253 Rubisco parameter were comparable among the Paniceae species tested within each C₃ and
254 C₄-subtype grouping (Table S3). This facilitated the derivation of averaged ΔH_a and scaling

255 constant values (c) for each parameter (Fig 3a). Consistent with the highly variable
256 properties of Rubisco from each Paniceae grouping (Fig 1) the ΔH_a values showed greater
257 variation (Fig 3a) than that reported for Rubisco from differing C₃ species¹⁸ and C₄-dicot
258 *Flaveria* species¹⁹. This divergence is readily apparent from plots using the averaged ΔH_a
259 values to extrapolate the temperature response of k_{cat}^c (Fig 3b), $K_C^{21\%O_2}$ (Fig 3c), $k_{cat}^c /$
260 $K_C^{21\%O_2}$ (Fig 3d) and $S_{C/O}$ (Fig 3e) for each Paniceae Rubisco grouping and tobacco
261 Rubisco (control).

262 The k_{cat}^c for each Rubisco showed a biphasic Arrhenius temperature response above
263 and below $\sim 25^\circ\text{C}$ (Fig S1). This necessitated the derivation of two ΔH_a and c
264 measurements for each Rubisco k_{cat}^c (Fig. 3a) whose modeled temperature responses
265 intersect at 25°C (Fig 3b). Importantly, the dual activation energy response of k_{cat}^c is
266 universal to all temperature response studies of plant Rubisco but mostly not
267 acknowledged^{15,18-20,28,30-32}. The basis for the asymmetric response remains uncertain.

268 At each assay temperature the k_{cat}^c and $K_C^{21\%O_2}$ for each NADP-ME and PCK
269 Rubisco were consistently ~ 2 -fold higher than Rubisco from *P. bisulcatum* (C₃), *P.*
270 *milioides* (C₂) and each NAD-ME species (Table S1 and S2). The shared change in k_{cat}^c
271 with temperature by NAD-ME and C₂-C₃ Rubisco (Fig 3b) was not evident in the measured
272 $K_C^{21\%O_2}$ values that showed a heightened rate of increase with temperature by NAD ME
273 Rubisco (Fig. 3c). The biphasic response of k_{cat}^c was evident in corresponding measures of
274 carboxylation efficiency ($k_{cat}^c / K_C^{21\%O_2}$) that showed two linear responses that deviated at
275 temperatures above and below $\sim 25^\circ\text{C}$ for each Rubisco (Fig 3d). A comparable k_{cat}^c / K_C
276 temperature dependency is apparent for the Rubisco from *Flaveria* C₃ and C₄ species¹⁹ and
277 *Setaria viridis* C₄-Rubisco¹⁵. The differential slopes of the linear regression underscores

278 the significant variation in k_{cat}^c and $K_C^{21\%O_2}$ between each Paniceae Rubisco grouping (both
279 below and above 25°C) and emphasizes the extrapolative limitations of kinetic surveys
280 examining only a few temperatures. This is particularly relevant for measures of $S_{C/O}$ where
281 the extent of exponential change appears more prevalent with reducing temperature (Fig.
282 3e).

283 **The potential for improving C₃-photosynthesis under current and future CO₂ and** 284 **elevated temperatures**

285 The temperature response of each Paniceae Rubisco showed varying extents of
286 improvement in $S_{C/O}$ and/or $k_{\text{cat}}^c/K_C^{21\%O_2}$ relative to tobacco Rubisco (Fig S3 and S4). The
287 improvements observed were greater for Rubisco from *P. bisulcatum* (C₃), *Urochloa*
288 *panicoides* (C₄-PCK) and *P. deustum* (C₄-PCK). When modeled in a C₃-photosynthesis
289 context under varying temperature and chloroplast CO₂ pressures (C_c) under saturating
290 illumination (Fig S5) all three Rubiscos differentially improved carbon assimilation
291 relative to tobacco Rubisco (Fig 4). At temperatures below 20°C the simulated
292 photosynthesis rates were limited by electron transport rate at atmospheric CO₂ (C_a) levels
293 above those of pre-industrial times ($C_a > 280$ ppm $\approx C_c > 170$ ppm) (Fig S5). Improvements
294 in $S_{C/O}$ were therefore required to enhance photosynthetic rates at low temperature, a
295 kinetic trait afforded by Paniceae C₃/C₂ Rubisco (Fig 3c), in particular *P. bisulcatum*
296 Rubisco (Fig 4 and S3). However, the heightened $S_{C/O}$ sensitivity of *P. bisulcatum* Rubisco
297 to increasing temperature (Fig S3a) caused these improved photosynthetic rates to wane
298 with increasing C_a and temperature (Figs 4 and S5). In contrast, the improved $S_{C/O}$ response
299 to temperature by *P. deustum* Rubisco (Fig S3) and rising $k_{\text{cat}}^c/K_C^{21\%O_2}$ (Fig S4)
300 substantially improved photosynthesis rates at temperatures $>20^\circ\text{C}$ under current and

301 future C_a levels (Fig 4b). This improvement exceeded that simulated for *U. panicoides*
302 Rubisco whose lower $S_{C/O}$ hindered its enhancement potential. The antagonistic advantage
303 of these Paniceae Rubisco to lower (*P. bisulcatum*) and higher (*U. panicoides*, *P. deustum*)
304 temperatures were not apparent from the 25°C kinetic measurements.

305 **The challenge of identifying catalytic switches in Paniceae Rubisco**

306 The *rbcL* gene in the plastome of each Paniceae species were fully sequenced and their
307 amino acid sequences compared (Fig 5a). A phylogenetic analysis revealed the L-subunit
308 sequences branched according to C_3 and C_4 -subtype physiology (Fig. S6) except *P.*
309 *monticola* (NADP-ME) and *M. maximus* (PCK) Rubisco that share identical L-subunits
310 but show large catalytic variation (Table S1 and S2). This suggests that Paniceae Rubisco
311 small subunits influence catalysis, a function likely shared by the small (S-) subunits of
312 sorghum³⁴ and wheat³⁵ Rubisco.

313 While examination of the S-subunit diversity among Paniceae remains to be
314 undertaken, our L-subunit analysis identified Ala 94 and Ala 228 (spinach Rubisco
315 numbering) as exclusive to C_4 Rubisco with Ser 328 and Glu 470 substitutions favored by
316 PCK and NADP-ME Rubisco (Fig 5a). Potential roles for amino acids 94 and 228 in
317 catalysis are unclear. Residue 94 is distal to the catalytic sites in the equatorial region of
318 Rubisco exposed to solvent where it facilitates interactions with Rubisco activase
319 (RCA)^{36,37}. Residue 228 is within the $\alpha 2$ helix also distal to the catalytic site but proximal
320 to residues at the interface of each L-subunit and two S-subunit βA - βB loops (Figure 5b).
321 Ala-228-Ser substitutions influence structural movements in these loops and can influence
322 kinetics via long range effects^{38,39}. Catalytic roles for Ser-328 and Glu-470 appear more
323 obvious. Amino acid 328 is located at the hinge of loop 6 that closes over the catalytic site

324 to facilitate intra-molecular interactions that influences both the fixation rate and partiality
325 for carboxylation or oxygenation⁴⁰. Loop 6 closure involves the L-subunit C-terminus
326 where amino acid 470 resides (Fig 5b). As a hydrophobic Ala-470 in the Panicaceae NAD-
327 ME and C₃ Rubisco, burial of the side chains into the enzyme surface may slow C-terminus
328 movement. In contrast, Glu/Gln-470 might enhance solvent exposure and increase C-
329 terminal tail mobility to alter the dynamics of loop 6 closure and stimulate k_{cat}^c .

330 We sought to test the possible role of L-subunit amino acid replacement(s) in
331 influencing the variability in kinetics and temperature response among Panicaceae Rubisco
332 by tobacco chloroplast transformation. Multiple chloroplast genome (plastome)
333 transformed tobacco lines were made (tob^{PdL} and tob^{PbL}) where the tobacco plastome *rbcL*
334 gene was replaced with the *rbcL* gene from *P. bisulcatum* or *P. deustum* were generated
335 (Fig S7a). Each transformed line was unable to survive outside of tissue culture (Fig 5c).
336 Despite producing ample levels of *Panicum rbcL* mRNA (Fig S7b), no hybrid L₈S₈
337 holoenzyme (comprising *Panicum* L-subunits and tobacco S-subunits, Fig S7c) or
338 unassembled *Panicum* L-subunits (Fig S7d) were detected. This suggests there are
339 incompatibilities in the biogenesis requirements (translation, folding and/or assembly) of
340 Rubisco between monocot and dicot species.

341 **Discussion:**

342 As calls for expanding the range of Rubiscos included in catalytic diversity studies
343 increase, so should the range of temperatures examined. Unlike prior C₃-focused Rubisco
344 diversity studies, our high resolution catalytic screen revealed variation in the kinetic
345 trajectories of Paniceae Rubisco capable of enhancing C₃-photosynthesis at temperatures
346 otherwise missed, or misjudged, from assaying at 25°C and one or two other temperatures.

347 Our analyses validate the co-evolution of higher k_{cat}^c and K_C across C₄-Rubiscos in
348 response to a CCM^{4,8,12,16,18,20}, and unveil the widest variability in temperature kinetics
349 reported for vascular plant Rubisco to date. We uniquely reveal alignment of Rubisco
350 kinetics with CCM biochemistry and Paniceae biogeography. For example, the higher k_{cat}^c
351 and K_C of the NADP-ME and PCK Paniceae Rubisco correlated with the forecast higher
352 BSC CO₂ levels in these C₄-subtypes relative to the NAD-ME and the CCM deficient C₃/C₂
353 species⁴¹. The slower decline in $S_{C/O}$ by PCK and NADP-ME Rubisco under increasing
354 temperature (Fig 3e) may reflect their warmer origins relative to the drier and cooler origins
355 of NAD-ME and C₃ grasses, respectively⁴². Endeavors to determine whether these
356 correlations extend to other C₄-species should take heed of inaccurately extrapolating the
357 response of k_{cat}^c to temperature using a single Arrhenius fit rather than correctly accounting
358 for its biphasic response that deviates at ~25°C (Fig 3b) – a relationship recognized 40
359 years ago³², but whose mechanistic origin remains an unsolved.

360 The clustering of carboxylase properties of Paniceae Rubisco according to
361 photosynthetic physiology contrasted with the more variable oxygenase activities (Fig 1i
362 & j) supporting assertions these competing reactions can evolve independently due to
363 differences in the mechanism and energy profile of their multi-step reactions²³. This

364 variability engenders natural kinetic diversity which, on the Rubisco superfamily scale, is
365 relatively restricted for C₃-Rubisco^{2,14,17,21,25,29 19,31}. In contrast the broad kinetic diversity
366 among Paniceae Rubisco presents opportunities for enhancing C₃-photosynthesis under
367 varying atmospheric CO₂ and temperature (Fig S5). In particular *P. bisulcatum* (C₃) and *P.*
368 *deustum* (PCK) Rubisco could distinctly improve C₃-photosynthetic potential under cooler
369 and warmer temperatures, respectively, relative to the standardized tobacco Rubisco
370 control (Fig 4) #wheat/rice. The simulated improvements stemmed from temperature
371 dependent enhancements in S_{C/O} and/or $k_{cat}^c / K_C^{21\%O_2}$ (Fig. 3d,e), and not necessarily from
372 high k_{cat}^c (as emphasized by⁸). Our findings suggest that improving C₃-crop photosynthesis
373 under warmer future climates may be best served by exploring the Rubisco kinetic diversity
374 of C₄-land plants, in particular among PCK and NADP-ME species.

375 Four L-subunit residues could contribute kinetic diversity among Paniceae
376 Rubisco. These included two amino acids within structural regions whose movements
377 influence Rubisco kinetics: the catalytic loop 6 (residue 328) and C-terminal tail (residue
378 470). Positive selection of Ala-328-Ser substitutions have been reported for some
379 *Limonium* haplotypes⁴³ and a few C₃ and CAM plant species¹⁷. This suggests the higher
380 k_{cat}^c and K_C of Paniceae NADP-ME and PCK Rubisco might arise from the Glu/Gln-470
381 substitution (Fig 5a). Our attempts to test this by heterologous expression in tobacco
382 chloroplasts proved unsuccessful (Fig 5c). The transformation limitation appears
383 associated with differences in the ancillary protein requirements of Paniceae Rubisco
384 biogenesis (Fig 5C), a constraint also preventing the production of Rubisco from red
385 algae⁴⁴ and seemingly other monocot species⁴⁵ in tobacco chloroplasts.

386 Our data indicate the S-subunits also likely influence the kinetic diversity among
387 Paniceae Rubisco. A comparable kinetic determining property was postulated for S-
388 subunits in rice and wheat Rubisco^{34,35}. In *P. virgatum* four *RbcS* mRNAs are made
389 (Phytozome) whose translated 121-123 amino acid S-subunits vary by 1 to 6 residues.
390 Mutagenic study of the multiple *RbcS* transcripts produced in Paniceae would be a
391 significant undertaking, but one possibly made easier using modern site specific nucleus
392 gene editing tools that are now available in a variety of crop species⁴⁶. Clarifying the
393 influence of S-subunits on the temperature kinetics of Rubisco from differing plant origins
394 is critical to developing appropriate L- and/or S-subunit mutagenic technologies for
395 modifying crop Rubisco kinetics to suit future climates.

396 Corresponding author for material requests is spencer.whitney@anu.edu.au

397 **Acknowledgements**

398 We thank Asaph Cousins for supplying their *S. viridis* Rubisco kinetic data for analysis.

399 This research was funded by the following grants from the Australian Research Council:

400 DE130101760 (RES), DP120101603 (OG, SMW) and CE140100015 (OG, SMW).

401 **Author contributions**

402 RS, OG and SMW designed the study and undertook the experimental work. MVK

403 undertook the phylogenetic analysis and LHG the structural analysis. All authors

404 contributed to drafting the paper.

405 **Competing financial interests**

406 The authors declare no competing financial interests.

407 **References**

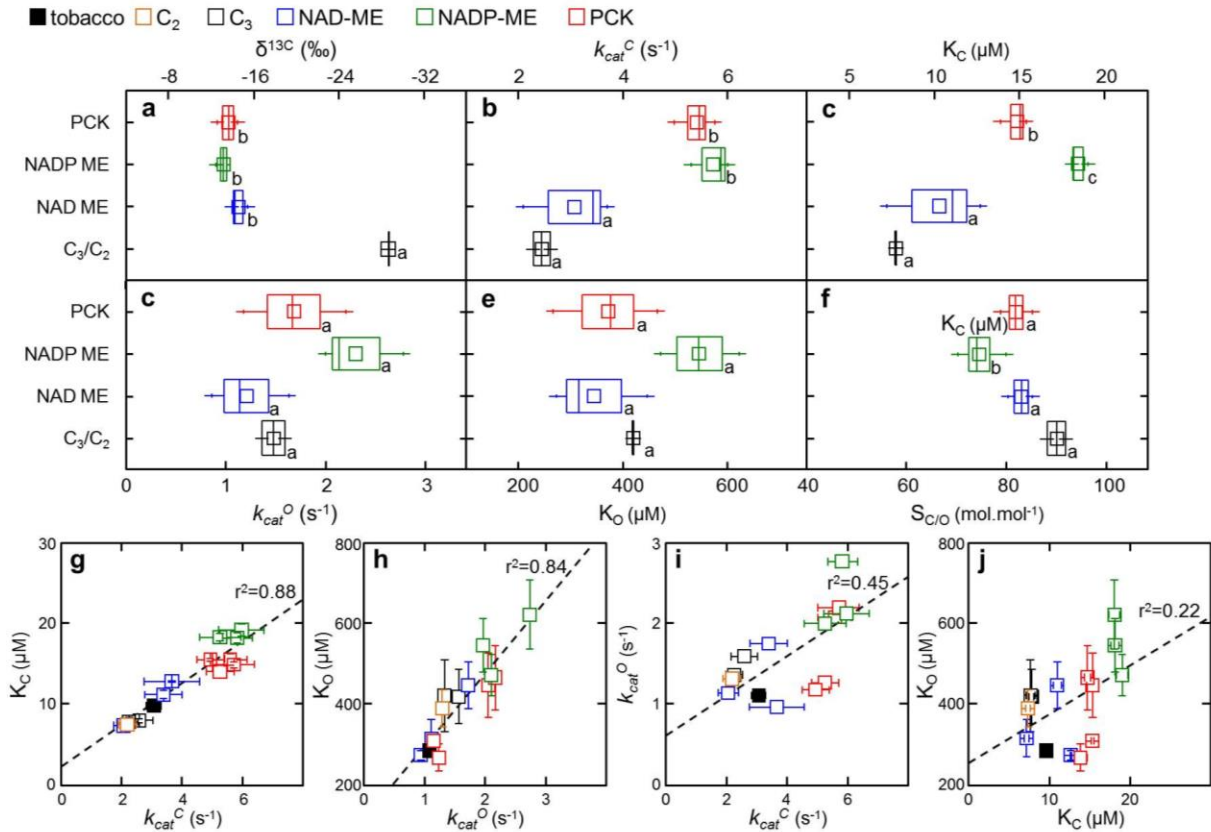
- 408 1 Ort, D. R. *et al.* Redesigning photosynthesis to sustainably meet global food and
409 bioenergy demand. *Proc Natl Acad Sci U S A* **112**, 8529-8536 (2015).
- 410 2 Zhu, X. G., Long, S. P. & Ort, D. R. Improving photosynthetic efficiency for greater
411 yield. *Annu Rev Plant Biol* **61**, 235-261 (2010).
- 412 3 Long, Stephen P., Marshall-Colon, A. & Zhu, X.-G. Meeting the global food
413 demand of the future by engineering crop photosynthesis and yield potential. *Cell*
414 **161**, 56-66 (2015).
- 415 4 Carmo-Silva, E., Scales, J. C., Madgwick, P. J. & Parry, M. A. J. Optimizing
416 Rubisco and its regulation for greater resource use efficiency. *Plant Cell Env* **38**,
417 1817-1832 (2015).
- 418 5 Evans, J. R. Improving photosynthesis. *Plant Physiol* **162**, 1780-1793 (2013).
- 419 6 Parry, M. A. J. *et al.* Rubisco activity and regulation as targets for crop
420 improvement. *J Exp Bot* **64**, 717-730 (2013).
- 421 7 von Caemmerer, S., Quick, W. P. & Furbank, R. T. The development of C₄ rice:
422 current progress and future challenges. *Science* **336**, 1671-1672 (2012).
- 423 8 Whitney, S. M., Houtz, R. L. & Alonso, H. Advancing our understanding and
424 capacity to engineer nature's CO₂-sequestering enzyme, Rubisco. *Plant Physiol*
425 **155**, 27-35 (2011).
- 426 9 Andersson, I. Catalysis and regulation in Rubisco. *J Exp Bot* **59**, 1555-1568 (2008).
- 427 10 Andersson, I. & Backlund, A. Structure and function of Rubisco. *Plant Physiol*
428 *Biochem* **46**, 275-291 (2008).
- 429 11 Sharwood, R. E., Ghannoum, O. & Whitney, S. M. Prospects for improving CO₂
430 fixation in C₃-crops through understanding C₄-Rubisco biogenesis and catalytic
431 diversity. *Curr Opin Plant Biol* **31**, 135-142 (2016).
- 432 12 Carmo-Silva, A. E. *et al.* Rubisco activities, properties, and regulation in three
433 different C₄ grasses under drought. *J Exp Bot* **61**, 2355-2366 (2010).
- 434 13 Galmes, J. *et al.* Expanding knowledge of the Rubisco kinetics variability in plant
435 species: environmental and evolutionary trends. *Plant Cell Environ* **37**, 1989-2001
436 (2014).
- 437 14 Galmés, J., Kapralov, M. V., Copolovici, L. O., Hermida-Carrera, C. & Niinemets,
438 Ü. Temperature responses of the Rubisco maximum carboxylase activity across
439 domains of life: phylogenetic signals, trade-offs, and importance for carbon gain.
440 *Photosynth Res* **123**, 183-201 (2015).
- 441 15 Jordan, D. B. & Ogren, W. L. The CO₂/O₂ specificity of ribulose 1,5-bisphosphate
442 carboxylase oxygenase - dependence on ribulosebisphosphate concentration, pH
443 and temperature. **161**, 308-313 (1984).
- 444 16 Prins, A. *et al.* Rubisco catalytic properties of wild and domesticated relatives
445 provide scope for improving wheat photosynthesis. *J Exp Bot* **67**, 1827-1838
446 (2016).
- 447 17 Young, J. N. *et al.* Large variation in the Rubisco kinetics of diatoms reveals
448 diversity among their carbon-concentrating mechanisms. *J Exp Bot* **67**, 3445-3456
449 (2016).

- 450 18 Andrews, T. J. & Whitney, S. M. Manipulating ribulose biphosphate
451 carboxylase/oxygenase in the chloroplasts of higher plants. *Arch.Biochem.Biophys.*
452 **414**, 159-169 (2003).
- 453 19 Raven, J. A. Rubisco: still the most abundant protein of Earth? *New Phytol* **198**, 1-
454 3 (2013).
- 455 20 Sage, R. F. The evolution of C₄ photosynthesis *New Phytol* **161**, 341-370 (2004).
- 456 21 Sage, R. F., Christin, P.-A. & Edwards, E. J. The C₄ plant lineages of planet Earth.
457 *J Exp Bot* **62**, 3155-3169 (2011).
- 458 22 Furbank, R. T. Evolution of the C₄ photosynthetic mechanism: are there really three
459 C₄ acid decarboxylation types? *J Exp Bot* **62**, 3103-3108 (2011).
- 460 23 Sage, R. F., Sage, T. L. & Kocacinar, F. Photorespiration and the evolution of C₄
461 photosynthesis. *Ann Rev Plant Biol* **63**, 19-47 (2012).
- 462 24 Ghannoum, O. *et al.* Faster rubisco is the key to superior nitrogen-use efficiency in
463 NADP-malic enzyme relative to NAD-malic enzyme C₄ grasses. *Plant Physiol* **137**,
464 638-650 (2005).
- 465 25 Sharwood, R., von Caemmerer, S., Maliga, P. & Whitney, S. The catalytic
466 properties of hybrid Rubisco comprising tobacco small and sunflower large
467 subunits mirror the kinetically equivalent source Rubiscos and can support tobacco
468 growth. *Plant Physiol* **146**, 83-96 (2008).
- 469 26 Sharwood, R. E., Sonawane, B. V., Ghannoum, O. & Whitney, S. M. Improved
470 analysis of C₄ and C₃ photosynthesis via refined in vitro assays of their carbon
471 fixation biochemistry. *J Exp Bot* **67**, 3137-3148 (2016).
- 472 27 Whitney, S. M. & Sharwood, R. E. Construction of a tobacco master line to improve
473 Rubisco engineering in chloroplasts. *J Exp Bot* **59**, 1909-1921 (2008).
- 474 28 Tcherkez, G. G. B., Farquhar, G. D. & Andrews, T. J. Despite slow catalysis and
475 confused substrate specificity, all ribulose biphosphate carboxylases may be
476 nearly perfectly optimized. *Proc Nat Acad Sci* **103**, 7246-7251 (2006).
- 477 29 Boyd, R. A., Gandin, A. & Cousins, A. B. Temperature response of C₄
478 photosynthesis: biochemical analysis of Rubisco, phosphoenolpyruvate
479 carboxylase and carbonic anhydrase in *Setaria viridis*. *Plant Physiol* **169**, 1850-
480 1861 (2015).
- 481 30 Perdomo, J. A., Cavanagh, A. P., Kubien, D. S. & Galmés, J. Temperature
482 dependence of in vitro Rubisco kinetics in species of *Flaveria* with different
483 photosynthetic mechanisms. *Photosynth Res* **124**, 67-75 (2015).
- 484 31 Sage, R. F. Variation in the k_{cat} of Rubisco in C₃ and C₄ plants and some
485 implications for photosynthetic performance at high and low temperature. *J Exp*
486 *Bot* **53**, 609-620 (2002).
- 487 32 Savir, Y., Noor, E., Milo, R. & Tlusty, T. Cross-species analysis traces adaptation
488 of Rubisco toward optimality in a low-dimensional landscape. *Proc Nat Acad Sci*
489 **107**, 3475-3480 (2010).
- 490 33 Percy, R. W. & Ehleringer, J. Comparative ecophysiology of C₃ and C₄ plants.
491 *Plant Cell Env* **7**, 1-13 (1984).
- 492 34 Tcherkez, G. The mechanism of Rubisco-catalyzed oxygenation. *Plant Cell Env*
493 **39**, 983-997 (2016).
- 494 35 Farquhar, G. D., von Caemmerer, S. & Berry, J. A. A biochemical model of
495 photosynthetic CO₂ assimilation in leaves of C₃ species. *Planta* **149**, 78-90 (1980).

- 496 36 Sharwood, R. E. & Whitney, S. M. Correlating Rubisco catalytic and sequence
497 diversity within C₃ plants with changes in atmospheric CO₂ concentrations. *Plant*
498 *Cell Env* **37**, 1981-1984 (2014).
- 499 37 Sharkey, T. D., Bernacchi, C. J., Farquhar, G. D. & Singaas, E. L. Fitting
500 photosynthetic carbon dioxide response curves for C₃ leaves. *Plant Cell Env* **30**,
501 1035-1040 (2007).
- 502 38 Walker, B., Ariza, L. S., Kaines, S., Badger, M. R. & Cousins, A. B. Temperature
503 response of *in vivo* Rubisco kinetics and mesophyll conductance in *Arabidopsis*
504 *thaliana*: comparisons to *Nicotiana tabacum*. *Plant Cell Env* **36**, 2108-2119 (2013).
- 505 39 Hermida-Carrera, C., Kapralov, M. V. & Galmés, J. Rubisco catalytic properties
506 and temperature response in crops. *Plant Physiol.*, doi:10.1104/pp.16.01846
507 (2016).
- 508 40 Orr, D. *et al.* Surveying Rubisco diversity and temperature response to improve
509 crop photosynthetic efficiency. *Plant Physiol.*, doi:10.1104/pp.16.00750 (2016).
- 510 41 Badger, M. R. & Collatz, G. J. Studies on the kinetic mechanism of RuBP
511 carboxylase and oxygenase reactions, with particular reference to the effect of
512 temperature on kinetic parameters. *Carnegie YB* **76**, 355-361 (1977).
- 513 42 Ishikawa, C., Hatanaka, T., Misoo, S., Miyake, C. & Fukayama, H. Functional
514 incorporation of sorghum small subunit increases the catalytic turnover rate of
515 Rubisco in transgenic rice *Plant Physiol* **156**, 1603-1611 (2011).
- 516 43 Hauser, T., Popilka, L., Hartl, F. U. & Hayer-Hartl, M. Role of auxiliary proteins
517 in Rubisco biogenesis and function. *Nat Plants* **1** (2015).
- 518 44 Wachter, R. M. *et al.* Activation of interspecies-hybrid Rubisco enzymes to assess
519 different models for the Rubisco-Rubisco activase interaction. *Photosynth Res* **117**,
520 557-566 (2013).
- 521 45 Spreitzer, R. J., Peddi, S. R. & Satagopan, S. Phylogenetic engineering at an
522 interface between large and small subunits imparts land-plant kinetic properties to
523 algal Rubisco. *Proc Natl Acad Sci* **102**, 17225-17230 (2005).
- 524 46 von Caemmerer, S. & Furbank, R. T. The C₄ pathway: an efficient CO₂ pump.
525 *Photosynth Res* **77**, 191-207, doi:10.1023/a:1025830019591 (2003).
- 526 47 Still, C. J., Pau, S. & Edwards, E. J. Land surface skin temperature captures thermal
527 environments of C₃ and C₄ grasses. *Glob Ecol Biogeog* **23**, 286-296 (2014).
- 528 48 Galmés, J. *et al.* Environmentally driven evolution of Rubisco and improved
529 photosynthesis and growth within the C₃ genus *Limonium* (Plumbaginaceae). *New*
530 *Phytol* **203**, 989-999 (2014).
- 531 49 Whitney, S. M. & Andrews, T. J. Plastome-encoded bacterial ribulose-1, 5-
532 bisphosphate carboxylase/oxygenase (RubisCO) supports photosynthesis and
533 growth in tobacco. *Proc Nat Acad Sci* **98**, 14738-14743 (2001).
- 534 50 Bortesi, L. & Fischer, R. The CRISPR/Cas9 system for plant genome editing and
535 beyond. *Biotech Adv* **33**, 41-52 (2015).

536

Figure 1



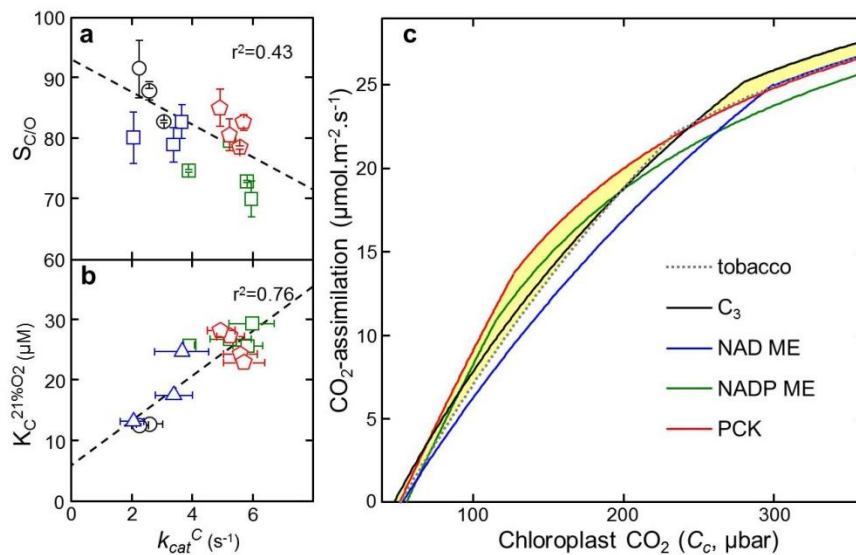
538

539 **Figure 1. The diversity in the catalytic properties of Rubisco at 25°C across C₃ and**
 540 **C₄ grasses within Paniceae.**

541 Box plots of comparative (a) leaf dry matter ¹²C/¹³C isotopic fractionation ($\delta^{13}C$) and (b to
 542 f) *in vitro* measured Rubisco kinetics from tobacco and Paniceae species with C₂, C₃ and
 543 varying C₄ subtypes (NADP ME, NAD ME and PCK). See Table S1 for species list.
 544 Median values shown in boxes as vertical line, 95% confidence limits represented by
 545 horizontal lines. Letter variation indicates significant differences ($p < 0.05$) between
 546 parameters (Table S1). Kinetic properties analyzed include (b) substrate saturated

547 carboxylation and (d) oxygenation turnover rates (k_{cat}^c , k_{cat}^o), the Michaelis constants (K_m)
 548 for (c) CO₂ and (e) O₂ (K_C , K_O) and (f) relative specificity for CO₂ over O₂ ($S_{C/O}$). (g to j)
 549 Pairwise relationships among the kinetic parameters to assess the quality of their linear
 550 correlations (dashed line).

Figure 2



551

552 **Figure 2. Variation among the Paniceae Rubisco kinetics differentially affect**
 553 **simulated rates of C₃-photosynthesis at 25°C.**

554 Comparison of the relationships between k_{cat}^c and either (a) $S_{C/O}$ or (b) $K_C^{21\%O_2}$, the value
 555 for K_C under ambient O₂ (O) calculated as $K_C(1+O/K_O)$ (Table S1). The r^2 values show the
 556 quality of their linear correlations (dashed lines). (c) The influence of the averaged
 557 Paniceae C₃ and C₄ subtype Rubisco kinetics (Table S1) on CO₂ assimilation rates (A) at
 558 25°C in a C₃-leaf as a function of C_c . Lines are modelled (Farquhar et al., (1980)) using the
 559 carboxylase activity limited assimilation equation:

560

$$A = \frac{(C_c \cdot s_c - 0.5 O/S_{c/o}) k_{cat}^c \cdot B}{C_c \cdot s_c + K(1 + O/K_o)} - R_d$$

561 using a CO₂ solubility in H₂O (*s_c*) of 0.0334M bar⁻¹, an *O* of 253 μM, a Rubisco content
562 (*B*) of 30 μmol catalytic sites.m² and a non-photorespiratory CO₂ assimilation rate (*R_d*) of
563 1 μmol.m⁻².s⁻¹. The light limited CO₂ assimilation rates (to the right of the symbols) were
564 modelled according to the equation:

565

$$A = \frac{(C_c \cdot s_c - 0.5 O/S_{c/o}) J}{4(C_c \cdot s_c + O/S_{c/o})} - R_d$$

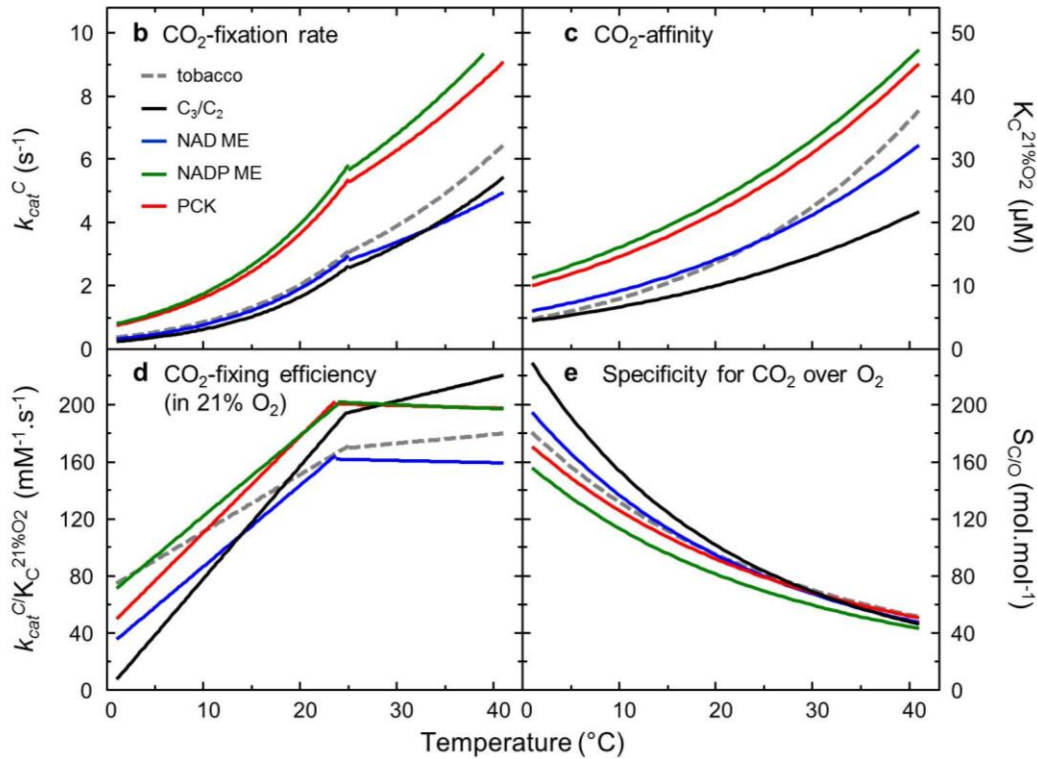
566 assuming an electron transport rate (*J*) of 160 μmol.m⁻².s⁻¹. Yellow shading indicates where
567 the modeled CO₂-assimilation rates of C₃, NADP-ME and PCK Paniceae Rubisco exceed
568 that of Rubisco from the model C₃-plant, tobacco (dotted line).

569

Figure 3

a

Rubisco grouping	# of species	$k_{cat}^C (< 25^\circ\text{C})$		$k_{cat}^C (> 25^\circ\text{C})$		$K_C^{21\%O_2}$		$S_{C/O}$	
		$\Delta H_a (\pm S.E.)$ (kJ mol ⁻¹)	$c (\pm S.E.)$	$\Delta H_a (\pm S.E.)$ (kJ mol ⁻¹)	$c (\pm S.E.)$	$\Delta H_a (\pm S.E.)$ (kJ mol ⁻¹)	$c (\pm S.E.)$	$\Delta H_a (\pm S.E.)$ (kJ mol ⁻¹)	$c (\pm S.E.)$
tobacco	n=1	60.3	25.5	36.4	15.8	37.3	17.9	22.5	-4.7
C ₃ /C ₂	n=2	69.8 ± 1.4 ^b	29.0 ± 0.6 ^b	36.3 ± 4.0 ^b	15.5 ± 1.5 ^b	28.2 ± 2.8 ^a	13.9 ± 1.1 ^a	28.6 ± 1.1 ^b	-7.1 ± 0.4 ^a
NAD ME	n=3	62.7 ± 4.5 ^{ab}	26.4 ± 1.6 ^a	27.6 ± 2.3 ^{ab}	12.2 ± 0.9 ^a	30.0 ± 4.4 ^a	15.0 ± 1.8 ^a	25.3 ± 1.6 ^{ab}	-5.8 ± 0.7 ^{ab}
NADP ME	n=3	56.0 ± 0.6 ^a	24.4 ± 0.2 ^a	27.7 ± 1.4 ^a	12.9 ± 0.5 ^a	25.8 ± 4.0 ^a	13.7 ± 1.6 ^a	22.8 ± 2.0 ^a	-5.0 ± 0.8 ^b
PCK	n=3	55.6 ± 2.8 ^a	24.1 ± 1.1 ^a	26.4 ± 1.0 ^a	12.3 ± 0.4 ^a	26.9 ± 2.4 ^a	14.1 ± 0.9 ^a	21.8 ± 0.5 ^a	-4.4 ± 0.2 ^b



570

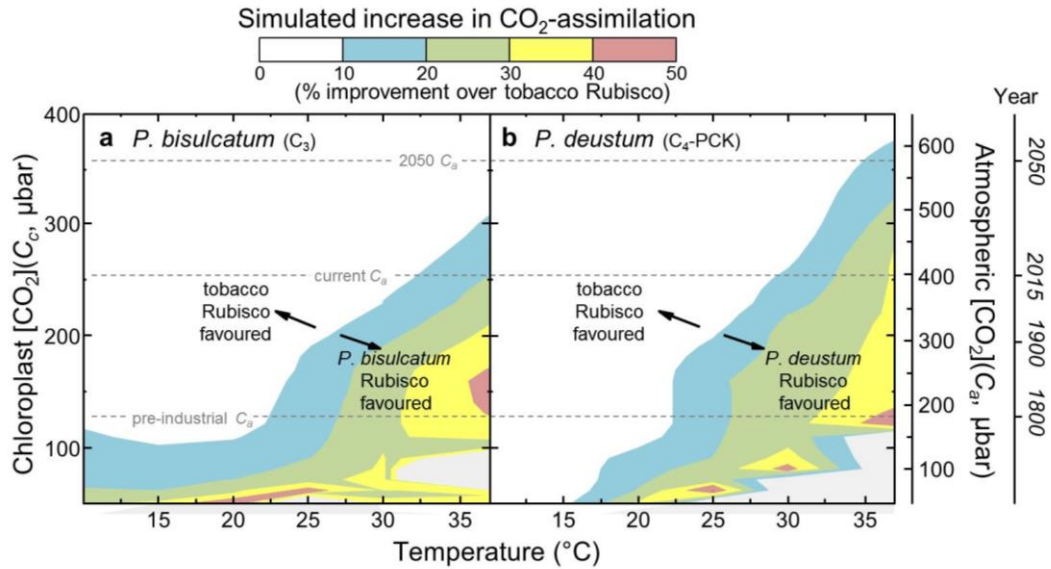
571 **Figure 3. Divergence in the catalytic properties of Paniceae and tobacco Rubisco in**
 572 **response to temperature.**

573 (a) The heat of activation (ΔH_a) and scaling constant (c) for the kinetic parameters of
 574 tobacco Rubisco and the mean ($\pm S.E.$) values measured for the various Paniceae species
 575 with C₄ (NAD ME, NADP ME, PCK) or C₃ (including the aligning C₂) biochemical
 576 physiologies (see Table S3). Letters show the statistical ranking using a post hoc Tukey
 577 test among the biochemical physiology groupings (different letters indicated differences at

578 the 5% level, $p < 0.05$). (**b to e**) Differences in the temperature response of tobacco (grey
579 dashed line) and the averaged kinetic properties for Rubisco from Paniceae species with
580 varying biochemical physiologies. The lines are derived as described in Figures S1 to S4
581 using the values listed in panel (**a**).

582

Figure 4



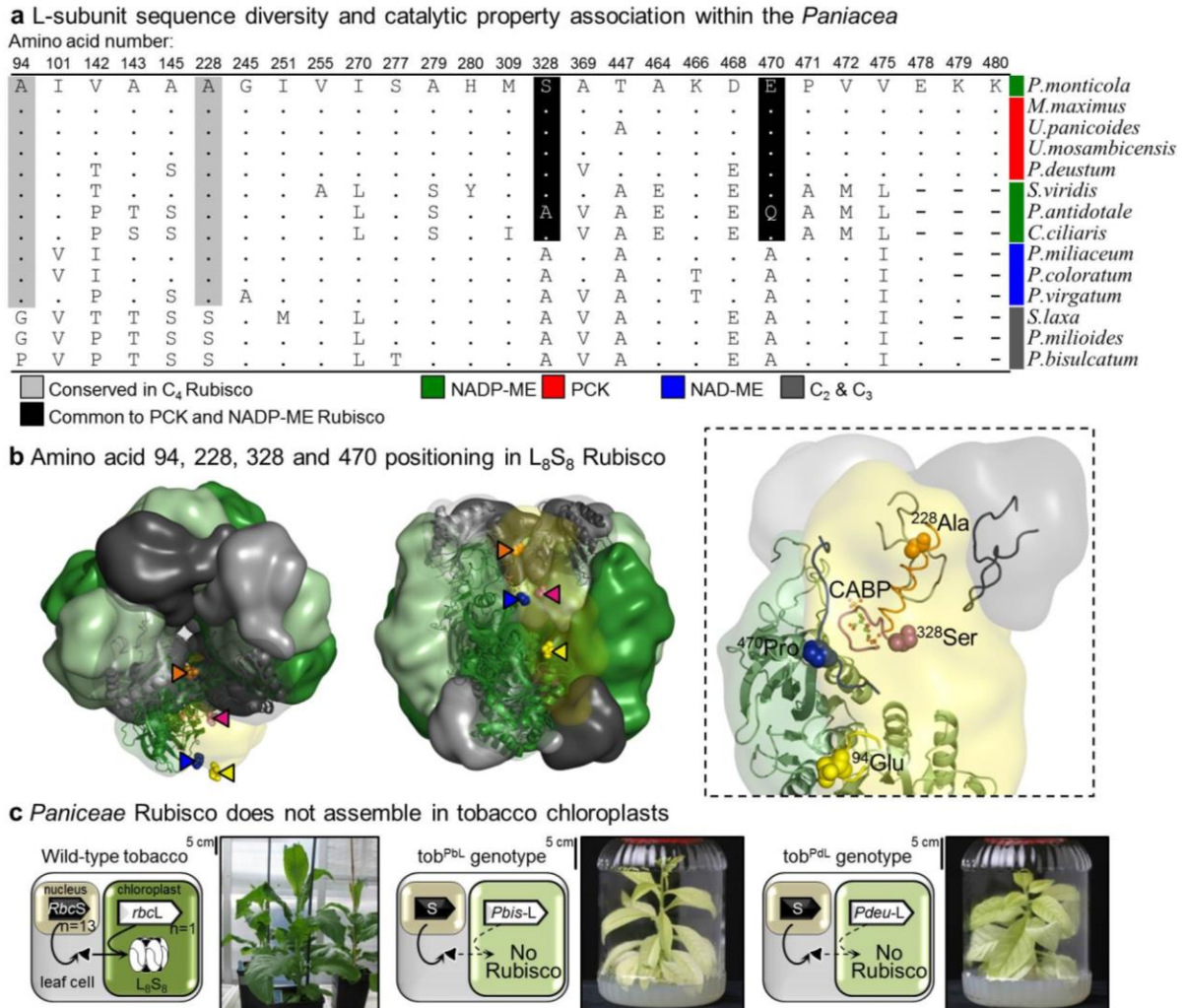
583

584 **Figure 4. The potential for improving the thermal response of C₃-photosynthesis.**

585 The benefits of (a) *P. bisulcatum* (C₃) and (b) *P. deustum* (C₄-PCK) Rubisco to the rate of
586 photosynthesis in a C₃-leaf under varying chloroplast CO₂ concentrations (C_a) and
587 temperature (see scale). Rate increases are presented as a percentage above that provided
588 by tobacco Rubisco. The data was modelled according to²⁴ using the parameters listed in
589 Table S4 and plotted in Fig S4.

590

Figure 5



591

592 **Figure 5. Approaches to decipher possible catalytic switches in the L-subunit of**
 593 ***Panicum* Rubisco.**

594 (a) Amino acid variation in the L-subunit of each *Panicum* Rubisco analysed in this study.

595 A phylogenetic analysis of the L-subunit sequences and their Genbank accession

596 information is provided in Figure S6. (b) Structure of spinach L₈S₈ Rubisco (L-subunits in

597 green, S-subunits grey) viewed from the top (left) and side (middle) showing the relative

598 locations of ⁹⁴Glu on the solvent-exposed Rubisco surface (yellow triangle), ²²⁸Ala in the
599 α 2 helix (orange triangle), ³²⁸Ser at the hinge of loop 6 (purple triangle) and ⁴⁷⁰Pro in the
600 C-terminal tail extension (blue triangle) of one L-subunit. A closer view of a L-subunit pair
601 (right) with one showing ribbon structural detail and the other showing the positioning of
602 ⁹⁴Glu, ²²⁸Ala, ³²⁸Ser and ⁴⁷⁰Pro relative to each other, an N-terminal domain loop, the α 2
603 helix, loop 6, C-terminal tail extension and S-subunit β A- β B loops (yellow, orange, purple,
604 blue and grey, respectively). An active site bound reaction-intermediate analogue 2-CABP
605 is shown as a ball and stick. (c) Chloroplast transformation of the Rubisco L-subunit genes
606 from *P. bisulcatum* (*Pbis-rbcL*) and *P. deustum* (*Pbis-rbcL*) into tobacco was undertaken
607 to identify the amino acids (catalytic switches) responsible for their differing catalytic
608 properties. No Rubisco biogenesis was detected in the tob^{PbL} and tob^{PdL} tobacco genotypes
609 produced. Accordingly these plants could only grow in tissue culture on sucrose containing
610 media and were highly chlorotic (as shown). Detailed analysis of the transformation,
611 Rubisco mRNA and protein biochemistry is provided in Figure S7.

612

613 **Supplemental data**

614 **Variation in response of C₃ and C₄ Paniceae Rubisco to temperature**
615 **provides opportunities for improving C₃ photosynthesis**

616 Robert E. Sharwood¹⁺, Oula Ghannoum^{2+*}, Maxim V. Kapralov^{1,3}, Laura H. Gunn^{1,4}, and
617 Spencer M. Whitney^{1+*}.

618 ¹Research School of Biology, Australian National University, Canberra ACT, 2601,
619 Australia.

620 ²Hawkesbury Institute for the Environment, Western Sydney University, Richmond
621 NSW, 2753, Australia.

622 ⁺ ARC Centre of Excellence for Translational Photosynthesis, Australian National
623 University Canberra ACT, 2601, Australia.

624 ³Current Address: School of Natural Sciences and Psychology, Liverpool John Moores
625 University, Liverpool, L3 3AF, United Kingdom.

626 ⁴Current address: Department of Cell and Molecular Biology, Uppsala University,
627 Uppsala, SE-751 24, Sweden.

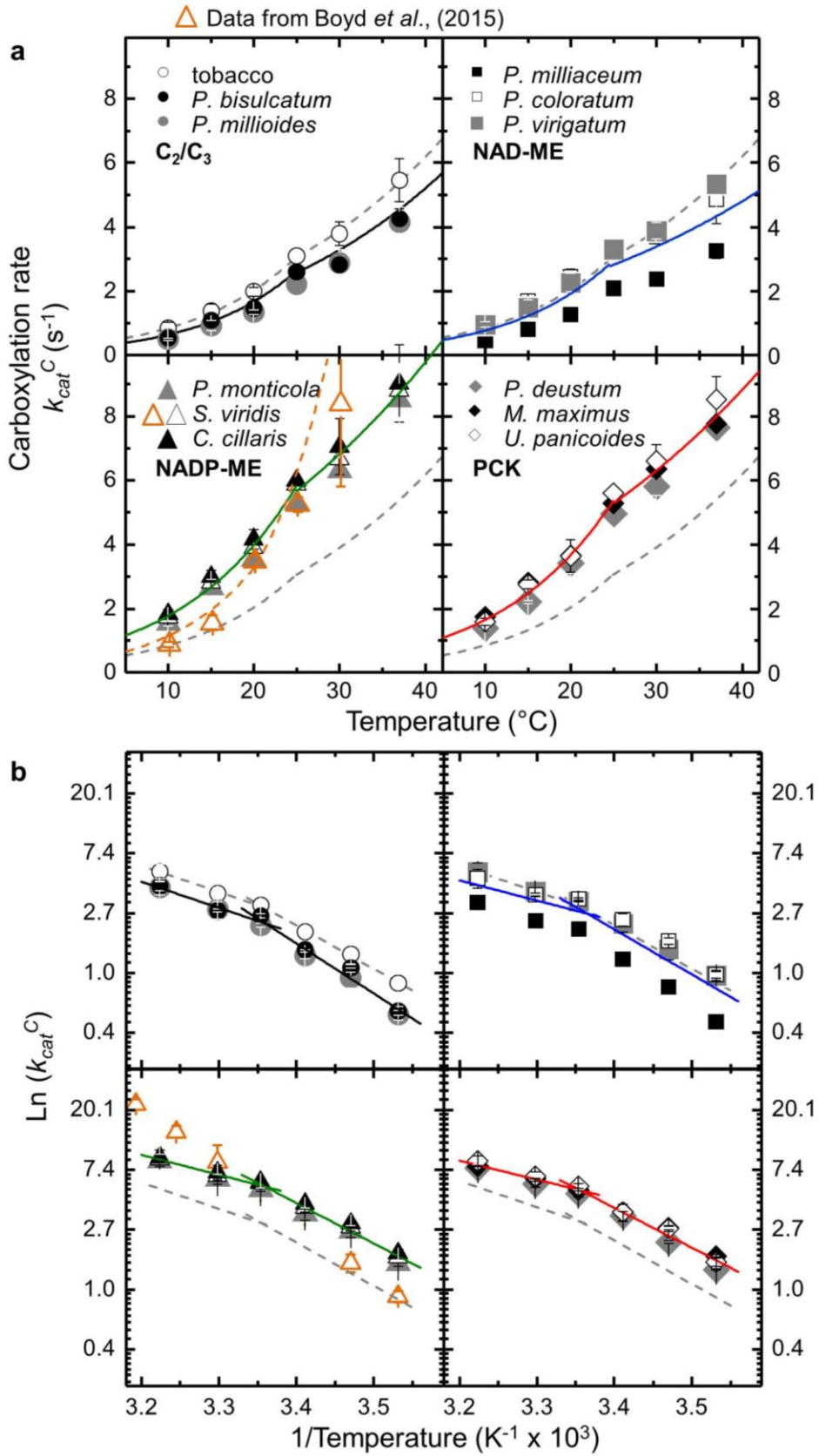
628 *Corresponding Authors: o.ghannoum@westernsydney.edu.au and
629 spencer.whitney@anu.edu.au

630

631 Number of Supplemental Figures: 7

632 Number of Supplemental Tables: 4

Supplementary Figure S1



634 **Figure S1. Variation in the temperature response of k_{cat}^c among the Paniceae and tobacco**
635 **Rubisco.**

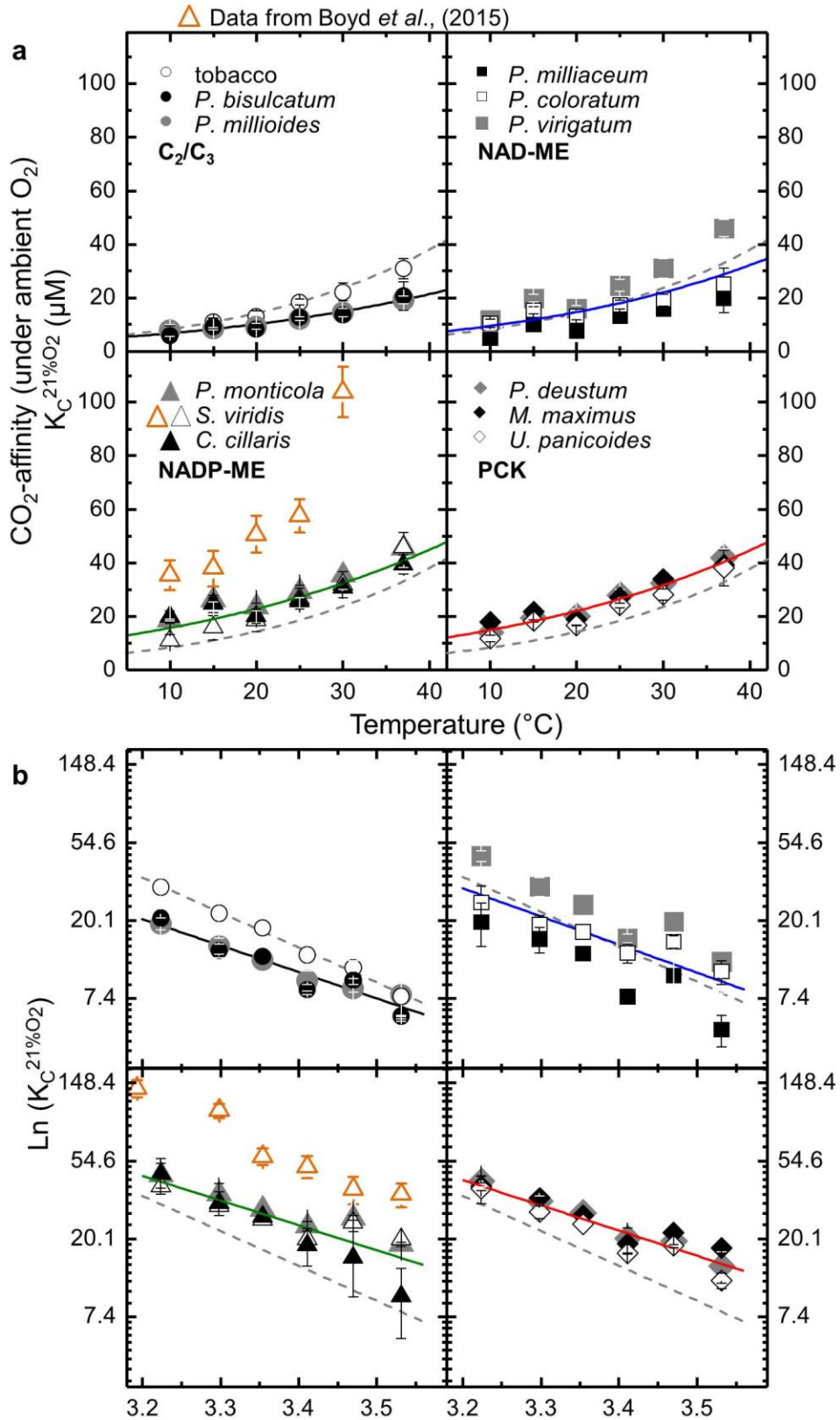
636 (a) Substrate saturated rates of carboxylation (k_{cat}^c) determined using soluble leaf protein extract ($n \geq 3$
637 biological samples per species) were measured at 10, 15, 20, 25, 30 and 37°C with the expected
638 exponential decrease in k_{cat}^c less evident at the lower assay temperatures for all Rubisco samples, as
639 evident in prior published data ^{18-20,28,30-32} }, including that of Boyd et al., (2015) ¹⁵ (orange triangles) for
640 *Seteria viridis* Rubisco measured by Membrane Inlet Mass Spectrometry (MIMS). Plotted data are listed
641 in Table S2. (b) Evaluation of the data via Arrhenius-style plots (*i.e.* $\ln k_{cat}^c$ vs $1/T$) indicated the k_{cat}^c
642 response diverged at around 25°C. Shown are the averaged linear fits to each Arrhenius plot in a biphasic
643 manner with the $< 25^\circ\text{C}$ measurements (*i.e.* at 10, 15, 20, 25°C) separated from the $> 25^\circ\text{C}$ measurements
644 (25, 30 and 37°C). The averaged data values were fitted to the following equation

645
$$Parameter = \exp \left[c - \frac{\Delta H_a}{RT} \right]$$

646 and the heat of activation (ΔH_a) for k_{cat}^c at both $< 25^\circ\text{C}$ and $> 25^\circ\text{C}$ was derived from the slope ($\ln(k_{cat}^c)$
647 $= -\Delta H_a/R$; where R is the molar gas constant, $8.314 \text{ J K}^{-1} \text{ mol}^{-1}$) and the scaling constant (c) from the
648 ordinal intercept. The calculated values are listed in Table S3 and were fitted to the above equation to
649 derive the exponential curves in panel a. For comparison, the fitted lines for tobacco Rubisco k_{cat}^c data
650 are shown as dotted lines in each C₄ Rubisco plot. See Table S3 for statistical analysis.

651

Supplementary Figure S2

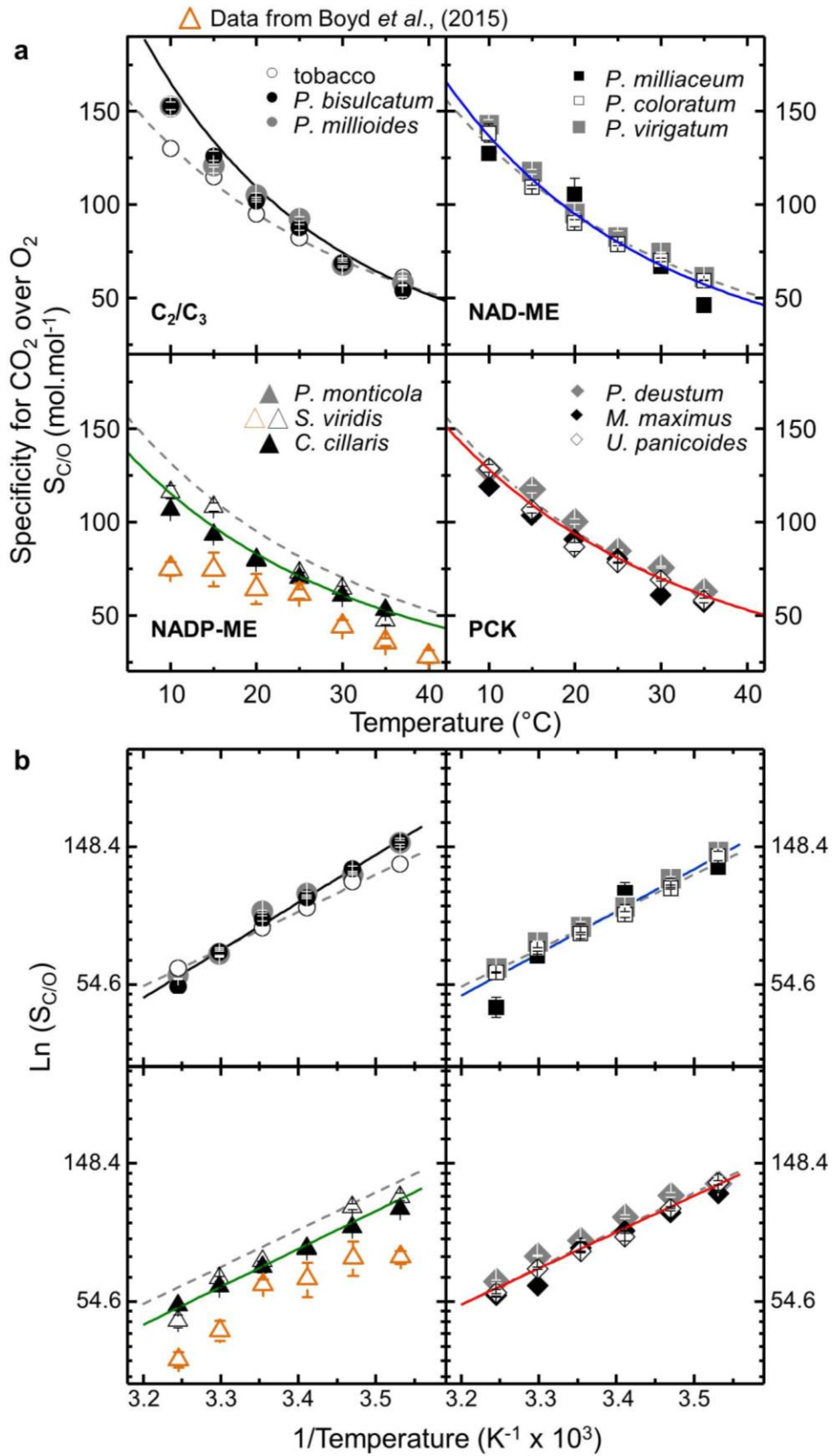


653 **Figure S2. Variation in the temperature response of CO₂ affinity among the Paniceae and tobacco**
654 **Rubisco.**

655 (a) The Michealis constant for CO₂ measured in the presence of ambient (253 μM) O₂ concentration
656 ($K_C^{21\%O_2}$) determined from the same assays used to determine k_{cat}^c in Fig S1 (n ≥ 3 biological samples
657 analyzed per specie) varied exponentially over 10 to 37°C. Orange triangles, data for *Seteria viridis*
658 Rubisco measured by MIMS¹⁵). Plotted data are listed in Table S2. (b) Arrhenius-style plots of the data
659 with the averaged linear regression fitted as described in Fig S1 to determine the heat of activation (ΔH_a)
660 and the scaling constant (c) values listed in Table S3 and used to derive the exponential curves shown in
661 panel (a). As a scaling comparison, the fitted lines for tobacco Rubisco $K_C^{21\%O_2}$ data are shown as dotted
662 lines in each C₄ Rubisco plot. See Table S3 for statistical analysis.

663

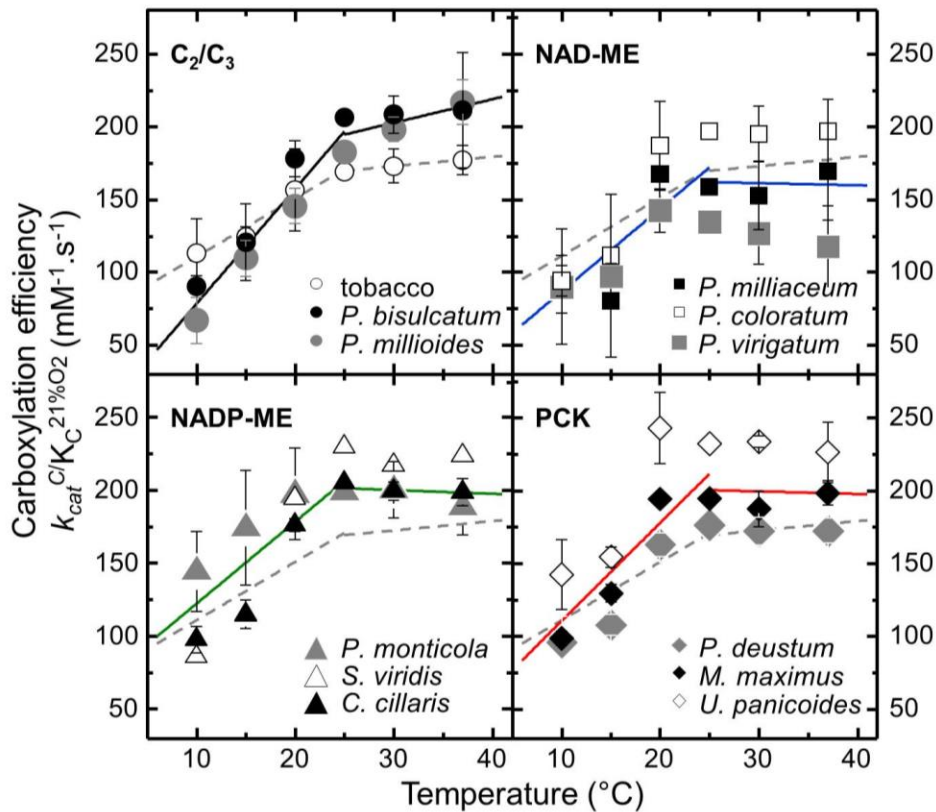
Supplementary Figure S3



665 **Figure S3. Variation in the temperature response of CO₂ over O₂ specificity among the Paniceae**
666 **and tobacco Rubisco**

667 (a) The influence of temperature on the specificity of CO₂ over O₂ ($S_{C/O}$) determined using Rubisco
668 purified from at least two biological samples per specie. Orange triangles, data for *Setaria viridis* Rubisco
669 measured by MIMS¹⁵. Plotted data are listed in Table S2. (b) Arrhenius plots of the data with the
670 averaged linear regression fitted as described in Fig S1 to determine the heat of activation (ΔH_a) and the
671 scaling constant (c) values for $S_{C/O}$ listed in Table S3 and used to derive the exponential curves shown in
672 panel (a). The fitted lines for tobacco Rubisco $S_{C/O}$ data are shown as dotted lines in each C₄ Rubisco
673 plot as a scaling comparison. See Table S3 for statistical analysis.

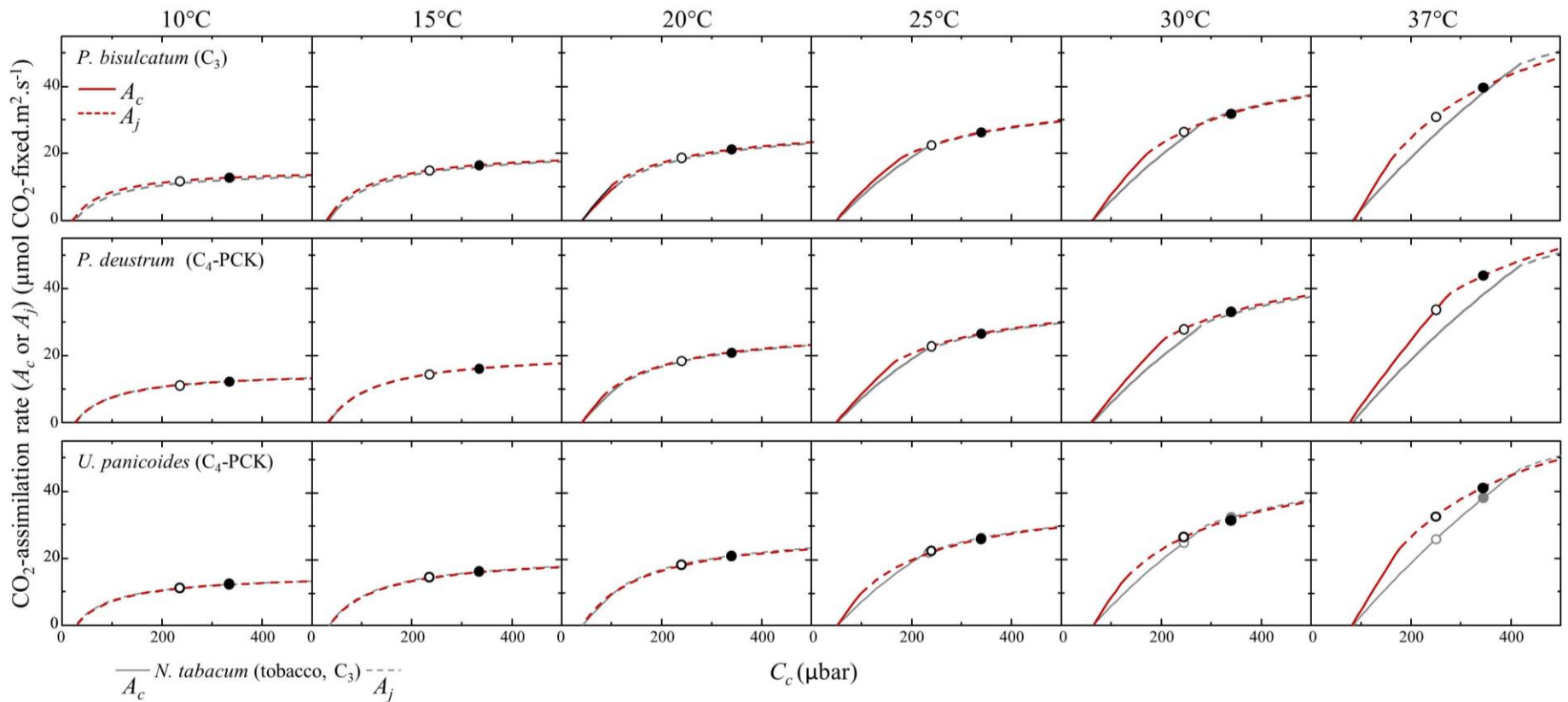
Supplementary Figure S4



674

675 **Figure S4. Variation in carboxylation efficiency under ambient O₂ among the Paniceae and**
 676 **tobacco Rubisco under varying temperature.**

677 The temperature response of carboxylation efficiency ($k_{cat}^c / K_C^{21\%O_2}$) for each Rubisco was calculated by
 678 dividing the averaged values of k_{cat}^c (FigS1) by its corresponding $K_C^{21\%O_2}$ values (Fig S2) for each assay
 679 temperature. As shown previously for *Flaveria*¹⁹ and *Seteria viridis*¹⁵ Rubisco, the carboxylation
 680 efficiency of each Paniceae and tobacco Rubisco declined at temperatures below 25°C and showed less
 681 variation at temperatures > 25°C. Shown are the linear regressions fitted to the averaged Paniceae data
 682 for each biochemical physiology. See Table S3 for statistical analysis.



683

684 **Figure S5. Effect of Rubisco kinetics on the thermal photosynthetic response.**

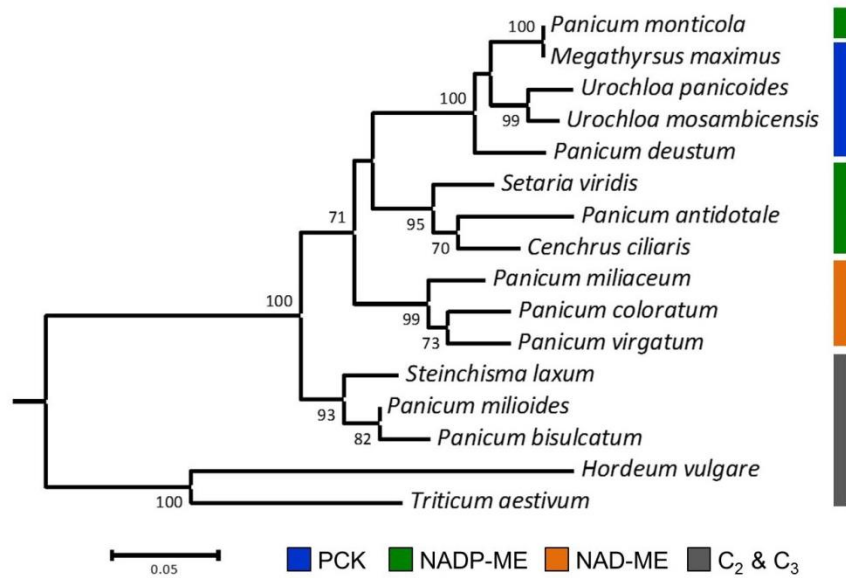
685 The effects Rubisco catalytic properties on the thermal response of leaf photosynthesis (A) to leaf chloroplastic CO₂ concentration (C_c).

686 The curves were modelled according to Farquhar *et al.* (1980)²⁴ using equations and parameters shown in Supplementary Table S5. The

687 solid and dashed lines refer to the Rubisco limited (A_c) and RuBP-regeneration limited (A_j) assimilation rates, respectively. The circles

688 refer to assimilation rates under current C_a (400 μ bar, white) and that predicted for 2050 (550 μ bar, black). Data for tobacco Rubisco
689 shown in grey in each panel for comparison.

Supplementary Figure S6

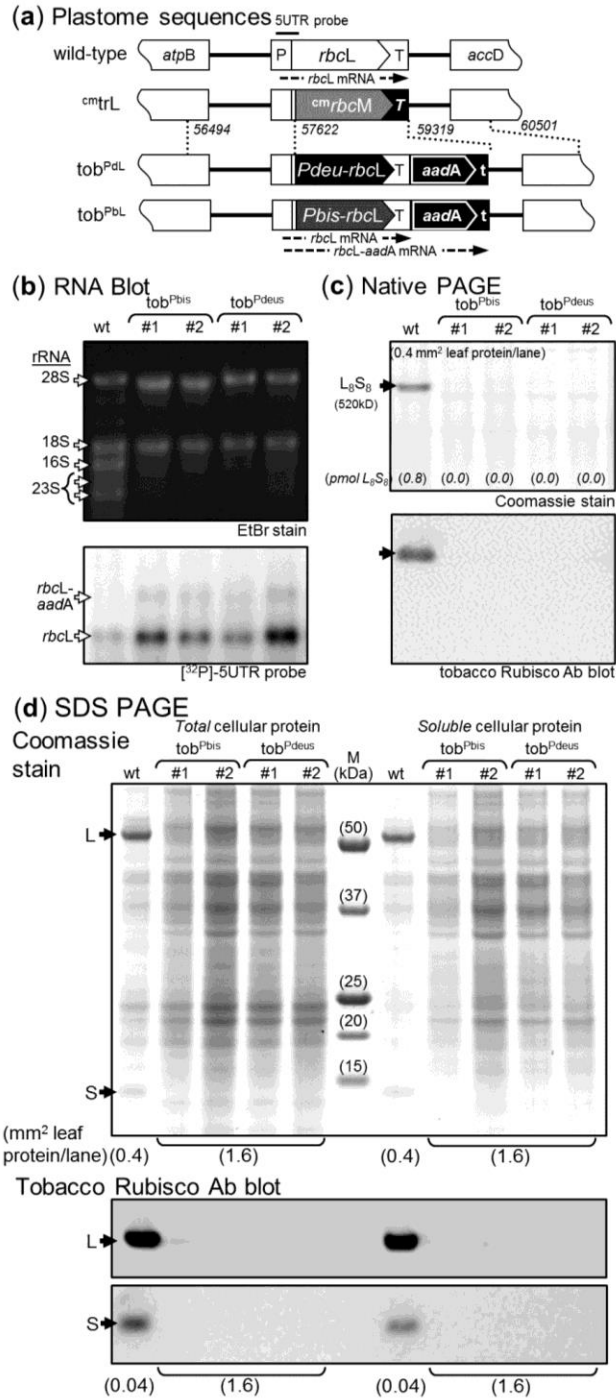


690

691 **Figure S6. Rubisco L-subunit phylogeny in the Paniceae.**

692 Maximum likelihood phylogeny of Rubisco L-subunit sequences from the fourteen Paniceae species
 693 examined in this study relative to the outgrouped Rubisco from *Hordeum vulgare* (barley) and *Triticum*
 694 *aestivum* (wheat). ML trees assembled under the Dayhoff model implemented in RAxML v.8⁴⁷ using
 695 translated L-subunit sequences from the full length *rbcL* genes available from the following Genbank
 696 accession: *P. bisulcatum*, (*); *S. laxa*, (*); *P. milioides*, (*); *P. antidotale*, (*); *P. monticola*, (*); *C.*
 697 *ciliaris*, (*); *S. viridis*, (KT289405.1); *P. virgatum*, (HQ731441.1); *P. milliaceum*, (KU343177.1); *P.*
 698 *coloratum*, (*); *M. maximus*, (*); *U. panicoides*, (*); *U. panicoides*, (*); *P. deustum*, (*); *U.*
 699 *mosambicensis*, (*); *H. vulgare*, (KT962228.1) and *T. aestivum*, (KJ592713.1). *sequences submitted to
 700 Genbank, awaiting accession numbers.

Supplementary Figure S7



702 **Figure S7. Chloroplast transformation of the *P. bisulcatum* (C₃) and *P. deustum* (C₄-PCK) *rbcL***
703 **genes to assess Paniceae Rubisco biogenesis in tobacco.**

704 (a) Comparison of the plastome sequence in wild-type, ^{cm}trL and the plastome transformed tob^{PbL} and
705 tob^{PdL} tobacco genotypes generated in this study. Duplicate tob^{PbL} and tob^{PdL} lines were made by
706 plastome transformation as described ¹³ by homologous recombination replacement of the ^{cm}*rbcM* gene
707 in the plastome of the ^{cm}trL tobacco genotype with *rbcL* genes for *P. bisulcatum* or *P. deustum* Rubisco
708 (synthesized to match the tobacco *rbcL* nucleotide sequence where feasible) and the *aadA* selectable
709 marker gene (coding resistance to spectinomycin). Numbering represents the flanking plastome
710 sequence in the pLEVpDL and pLEVpBL transforming plasmids. P, 292-bp *rbcL* promoter/5'UTR; T,
711 288-bp*rbcL* 3'UTR; T, 112-bp of *psbA* 3'UTR; t, 147-bp *rps16* 3'UTR. Position of the 221-bp 5UTR
712 probe ¹³ and the corresponding *rbcL* and *rbcL-aadA* mRNAs (dashed lines) to which it hybridizes are
713 indicated. (b) Total leaf RNA (5µg) extracted from tissue culture grown plant samples was separated on
714 denaturing formaldehyde gels and the EtBr stained RNA visualised (upper panel) before blotting onto
715 Hybond-N nitrocellulose membrane (GE healthcare) as described ¹¹ and probed with the ³²P-labelled
716 5UTR probe (lower panel). The probe correctly hybridised to the wild-type tobacco *rbcL* mRNA and the
717 *rbcL* and *rbcL-aadA* mRNA transcripts in each tob^{PbL} and tob^{PdL} line. (c) Soluble leaf protein from the
718 same leaves analyzed in (b) was processed for measuring Rubisco levels by NdPAGE analysis and ¹⁴C-
719 CABP quantification as described ²⁵. While wildtype tobacco L₈S₈ Rubisco was readily detected by ¹⁴C-
720 CABP binding, Coomassie staining and by immunoblot analysis with an antibody to tobacco Rubisco
721 following ndPAGE, these methods detected no hybrid L₈S₈ Rubisco biogenesis in the tob^{PbL} and tob^{PdL}
722 genotypes (*i.e.* complexes comprising the introduce *Panicum* L-subunits and the endogenous, cytosol
723 made tobacco S-subunits). (d) Further inspection of the soluble and total (comprising soluble + insoluble)
724 leaf protein separated by SDS PAGE did not detect any Rubisco L-subunit (~50 kDa) or S-subunit (~14.5

725 kDa) in either cellular protein fraction of the tob^{PbL} or tob^{PdL} lines by Comassie staining or Rubisco
726 antibody blot analysis. This indicated that even when grown in tissue culture the resource limitations
727 confronting the photosynthetically deplete tob^{PbL} and tob^{PdL} lines precluded the synthesis and /or
728 accumulation of *Panicum* sp. Rubisco L-subunits. Whether co-expressing their cognate SSu or/and Raf1
729 ⁴⁸ can circumvent this biogenesis challenge remains to be tested.

Table S1: Summary of the catalytic parameters of Paniceae and tobacco Rubisco at 25°C.

Species	Physiology	$\delta^{13}\text{C}$	k_{cat}^c	K_C	$K_C^{21\% \text{ O}_2}$	k_{cat}^o	K_O	k_{cat}^o/K_O	$S_{C/O}$	$k_{cat}^c/K_C^{21\% \text{ O}_2}$	k_{cat}^o/K_C
		(‰)	(s ⁻¹)	(μM)	(μM)	(s ⁻¹)	(μM)	(mM ⁻¹ .s ⁻¹)	(mol.mol ⁻¹)	(mM ⁻¹ .s ⁻¹)	(mM ⁻¹ .s ⁻¹)
Paniceae species	<i>Panicum antidotale</i>	-12.92	3.9 ± 0.2	n.m	25.2	n.m	n.m	n.m	74.5 ± 0.4	156	n.m
	<i>Panicum monticola</i>	-13.53	5.3 ± 0.7	18.2 ± 0.5	26.6	2.0	543 ± 67	3.7	79.4 ± 1.7	198	290
	<i>Cenchrus ciliaris</i>	-12.46	6.0 ± 0.8	19.0 ± 0.7	29.2	2.1	470 ± 52	4.5	69.9 ± 3.0	205	314
	<i>Setaria viridis</i>	-13.81	5.9 ± 0.5	18.1 ± 0.6	25.5	2.8	619 ± 86	4.4	72.7 ± 0.2	230	323
	<i>Panicum virgatum</i>	-13.98	3.3 ± 0.9	12.7 ± 0.1	24.5	0.9	271 ± 12	3.1	82.6 ± 2.8	133	258
	<i>Panicum milliaceum</i>	-15.50	2.1 ± 0.3	7.2 ± 0.3	13.1	1.1	313 ± 46	3.6	79.9 ± 4.3	159	287
	<i>Panicum coloratum</i>	-14.20	3.4 ± 0.6	11.1 ± 0.5	17.3	1.6	445 ± 58	3.6	84.8 ± 2.8	197	308
	<i>Megathyrsus maximus</i>	-14.32	5.3 ± 0.5	13.9 ± 0.8	27.1	1.3	265 ± 34	4.7	80.3 ± 2.8	195	380
	<i>Urochloa panicoides</i>	-14.51	5.6 ± 0.6	15.4 ± 0.7	24.1	2.1	444 ± 80	4.6	78.3 ± 0.3	232	364
	<i>Panicum deustum</i>	-12.62	5.0 ± 0.5	15.4 ± 0.2	28.1	1.2	306 ± 16	3.8	84.8 ± 0.2	177	322
	<i>Urochloa mosambicensis</i>	-13.08	5.7 ± 0.7	14.8 ± 0.4	22.8	2.2	464 ± 79	4.7	82.5 ± 1.3	252	388
	<i>Panicum milioides</i>	-31.50	2.2 ± 0.3	7.4 ± 0.3	12.1	1.3	387 ± 46	3.3	92.3 ± 1.0	182	301
	<i>Panicum bisulcatum</i>	-28.68	2.6 ± 0.4	7.8 ± 0.3	12.6	1.6	416 ± 67	3.8	87.7 ± 1.5	207	333
	<i>Steinchisma laxa</i>	-28.70	2.3 ± 0.3	7.7 ± 0.5	12.4	1.4	419 ± 89	3.2	91.4 ± 4.8	184	294
<i>Nicotiana tabacum</i>	n.m.	3.1 ± 0.3	9.7 ± 0.1	18.3	1.1	283 ± 15	3.9	82.6 ± 0.8	168	318	
Averages of parameters for Paniceae Rubisco	C ₃	-28.7±0.1 a	2.4±0.2 a	7.8±0.1 a	12.5±0.1 a	1.5±0.1 a	418±1 a	3.5±0.3 a	90±2 a	195±12 a	313±19 ab
	NAD-ME	-14.6±0.5 b	2.9±0.4 a	10.3±1.6 a	18.3±3.3 a	1.2±0.2 a	343±52 a	3.4±0.2 a	82±1 a	163±18 a	284±15 a
	NADP-ME	-13.3±0.4 b	5.7±0.2 b	18.4±0.3 c	27.1±1.1 b	2.3±0.2 a	544±43 a	4.2±0.3 a	74±3 b	211±10 a	309±10 ab
	PCK	-13.6±0.5 b	5.4±0.2 b	14.9±0.4 b	25.5±1.2 b	1.7±0.3 a	370±49 a	4.5±0.2 a	81±1 a	214±17 a	363±15 b
Type (p)		***	***	***	**	ns(0.08)	ns(0.072)	*	**	ns	*

731 For each species data are the mean±SE of at least N=3 biological samples assayed in duplicate. One-way ANOVA was undertaken
732 using the photosynthetic type/subtype as the main factor. Symbols show the statistical significance levels (ns = $p > 0.05$; * = $p < 0.05$;
733 ** = $p < 0.01$; ***: $p < 0.001$), while letters show the ranking of the means using a post hoc Tukey test (different letters indicate
734 statistical differences at the 5% level, $p < 0.05$). k_{cat}^o , maximal oxygenation rate calculated from $S_{C/O} = (k_{cat}^c / K_C) / (k_{cat}^o / K_O)$. $K_C^{21\% \text{ O}_2}$,
735 K_C under ambient atmospheric O₂ levels ($O = 252 \mu\text{M O}_2$ in air saturated H₂O) calculated as $K_C(1+O/K_O)$. n.m, not measured.

Table S2: The catalytic parameters of Paniceae and tobacco Rubisco between 10°C and 37°C.

Temp (°C)	tobacco N = 4 (x2)	<i>P. bis.</i> N = 3 (x2)	<i>P. milioid.</i> N = 3 (x2)	C2/C3	<i>P. miliac</i> N = 4 (x2)	<i>P. color</i> N = 3 (x2)	<i>P. virg</i> N = 3 (x2)	NAD ME	<i>P. mont.</i> N = 4 (x2)	<i>S. virid</i> N = 3 * <i>Boyd et.</i> <i>al 2015</i>	<i>C. ciliaris</i> N = 3 (x2)	NADP ME	<i>P. deust</i> N = 4 (x2)	<i>M. max</i> N = 3 (x2)	<i>U. panic</i> N = 3 (x2)	PCK	
k_{cat}^C (s ⁻¹)																	
10	0.88±0.19	0.53±0.04	0.49±0.04	0.51±0.02	0.44±0.01	0.97±0.06	0.96±0.08	0.79±0.17	1.52±0.06	1.70±0.03	<i>0.88±0.08</i>	1.81±0.14	1.68±0.08	1.40±0.02	1.75±0.04	1.58±0.11	1.58±0.10
15	1.37±0.22	1.09±0.07	0.92±0.15	1.00±0.08	0.79±0.06	1.70±0.09	1.48±0.24	1.32±0.27	2.64±0.27	2.80±0.15	<i>1.55±0.23</i>	2.99±0.17	2.81±0.10	2.21±0.05	2.80±0.10	2.75±0.14	2.59±0.19
20	1.98±0.13	1.47±0.02	1.34±0.07	1.40±0.07	1.26±0.01	2.43±0.24	2.27±0.29	1.99±0.37	3.54±0.37	3.88±0.24	<i>3.47±0.17</i>	4.15±0.31	3.86±0.18	3.42±0.31	3.65±0.02	3.64±0.50	3.57±0.08
25	3.10±0.08	2.60±0.19	2.21±0.09	2.41±0.20	2.08±0.05	3.41±0.09	3.30±0.06	2.93±0.43	5.28±0.16	5.85±0.33	<i>5.21±0.22</i>	5.98±0.09	5.70±0.21	4.96±0.32	5.38±0.12	5.60±0.26	5.28±0.18
30	3.78±0.37	2.83±0.07	2.87±0.41	2.85±0.02	2.37±0.12	3.70±0.11	3.87±0.26	3.31±0.48	6.29±0.51	6.65±0.29	<i>8.33±2.82</i>	7.04±0.87	6.66±0.22	5.80±0.28	6.34±0.13	6.59±0.51	6.25±0.23
37	5.45±0.67	4.26±0.30	4.15±0.47	4.20±0.06	3.24±0.24	4.86±0.77	5.34±0.90	4.48±0.64	8.49±1.03	8.78±0.28	<i>13.88±1.35</i> (35°C)	9.01±1.21	8.76±0.15	7.64±0.43	7.76±0.16	8.51±0.71	7.97±0.27
$K_C^{21\%O_2}$ (µM)																	
10	7.6±1.9	5.9±0.1	7.7±2.2	6.8±0.9	4.9±1.0	10.4±1.5	11.8±3.9	9.0±2.1	11.0±2.1	19.8±2.3	<i>35.4±5.5</i>	18.6±0.4	16.5±2.8	14.1±2.8	17.8±0.5	11.7±1.1	14.6±1.8
15	11.0±1.4	9.3±2.6	8.4±0.4	8.8±0.5	9.8±0.6	15.2±1.3	19.7±1.4	14.9±2.8	15.8±4.5	24.6±3.2	<i>37.9±6.7</i>	26.1±0.8	22.2±3.2	19.5±2.1	21.6±0.3	18.2±0.4	19.8±1.0
20	12.9±2.0	8.3±0.6	9.2±1.2	8.8±0.5	7.5±0.2	13.2±1.6	15.9±1.0	12.2±2.5	18.4±4.3	20.0±2.4	<i>50.6±7.0</i>	23.6±1.5	20.7±1.5	20.1±2.8	18.8±0.3	16.6±0.1	18.5±1.0
25	18.3±0.9	12.6±1.0	12.1±0.8	12.4±0.3	13.1±1.1	17.3±1.7	24.5±2.1	18.3±3.3	26.6±4.0	25.5±2.0	<i>57.5±6.3</i>	29.2±2.3	27.1±1.1	28.1±2.0	27.1±1.1	24.1±1.0	26.4±1.2
30	22.0±3.4	13.6±1.2	14.4±1.4	14.0±0.4	15.7±2.5	19.1±2.3	30.1±3.7	21.9±4.6	31.7±4.8	30.6±2.0	<i>103.8±9.4</i>	35.4±5.4	32.6±1.5	32.5±2.3	33.9±2.3	28.2±2.2	31.5±1.7
37	30.8±3.8	20.6±5.3	19.2±0.15	19.9±0.8	19.6±5.3	25.1±6.0	45.9±3.3	30.2±8.0	45.8±5.4	39.3±3.6	<i>138.1±15.3</i> (35°C)	45.6±7.2	43.5±2.1	42.0±3.0	39.2±2.0	38.0±6.6	39.7±1.2
$k_{cat}^C / K_C^{21\%O_2}$ (mM ⁻¹ .s ⁻¹)																	
10	111	90	64	77±13	90	93	81	88±4	138	86	26	97	107±16	99	98	135	111±12
15	125	117	110	114±3	81	111	75	89±11	167	114	42	115	132±17	113	129	152	131±11
20	154	178	144	161±17	167	185	142	165±12	192	194	73	176	189±6	170	194	219	194±14
25	169	206	183	194±12	159	197	135	164±18	198	229	93	205	211±9	177	195	232	201±16
30	172	208	200	203±4	151	194	125	156±20	198	217	81	199	205±6	179	187	234	200±17
37	177	206	217	211±5	165	194	116	158±23	186	223	104 (35°C)	198	202±11	182	198	224	201±12
$S_{C/O}$ (mol.mol ⁻¹)																	
	N = 4 (x3)	N = 2 (x3)	N = 2 (x3)		N = 2 (x3)	N = 3 (x3)	N = 2 (x3)			N = 2 (x3)		N = 2 (x3)		N = 3 (x3)	N = 2 (x3)	N = 2 (x3)	
10	130.0±1.0	152.7±2.0	152.4±4.9	152.5±0.1	127.1±2.6	138.2±5.1	142.7±2.6	136.0±4.7	n.m.	115.9±3.3	<i>74.9±3.6</i>	106.4±0.8	111.2±3.9	128.0±6.4	119.0±2.9	128.6±2.0	125.2±3.1
15	114.7±2.1	126.1±2.4	120.8±0.8	123.4±2.7	114.7±2.6	109.3±0.8	117.5±1.4	113.8±2.4		108.0±2.2	<i>74.5±9.1</i>	93.2±0.8	100.6±6.0	117.7±2.0	103.4±3.3	106.5±1.6	109.2±4.3
20	94.9±0.4	102.0±0.6	105.1±1.2	103.5±1.6	105.7±8.4	90.1±1.9	95.4±0.5	97.0±4.6		79.1±0.5	<i>64.1±7.9</i>	79.9±0.1	79.5±0.3	100.3±1.3	90.7±0.5	86.7±2.4	92.6±4.0
25	82.0±0.6	87.7±1.5	92.3±1.0	90.0±2.3	80.0±4.3	78.8±0.8	82.6±3.3	80.4±1.1		72.7±0.2	<i>61.5±2.5</i>	69.9±2.0	71.3±1.2	84.8±0.2	80.3±2.8	78.2±0.3	81.1±1.9
30	69.0±2.1	68.6±1.4	67.7±1.4	68.2±0.4	67.0±0.6	70.2±0.9	74.3±0.2	70.5±2.1		64.2±1.1	<i>35.6±2.0</i>	60.6±0.1	62.4±1.3	75.7±0.3	60.9±2.4	69.0±0.6	68.5±4.3
35	61.1±0.7	53.7±3.2	58.1±1.7	55.9±2.2	46.1±3.4	59.4±0.3	61.2±1.1	55.6±4.8		47.1±2.2	<i>27.8±3.4</i>	52.8±0.5	49.9±2.3	62.9±0.7	56.9±0.8	58.0±1.4	59.3±1.8

737 Rubisco catalysis parameters (average ± S.E.) measured in duplicate (x2) or triplicate (x3) for each biological sample (N). *Data for *S.*

738 *viridis* Rubisco shown in blue italic (N=4 ± S.E.) measured by MIMS¹⁵. The data for each species are plotted in Figures S1 to S4 with

739 the parameter averages (± SE) for tobacco Rubisco and for each Paniceae photosynthetic type/subtype shown in bold and shaded grey

740 are plotted in Figures 3. n.m, not measured. The data from this study are statistically analyzed following derivation of the heat of
741 activation (ΔH_a) and scaling constant (c) values for each parameter (see Table S3).

742
743

Table S3. Heat of activation (ΔH_a) and scaling constant (c) values among Paniceae and tobacco Rubisco kinetic parameters.

Species	Physiology	$k_{cat}^c (>25^\circ\text{C})$		$k_{cat}^c (<25^\circ\text{C})$		$K_C^{21\% \text{ O}_2}$		$S_{C/O}$	
		$\Delta H_a (\pm \text{S.D})$	$c (\pm \text{S.D})$	$\Delta H_a (\pm \text{S.D})$	$c (\pm \text{S.D})$	$\Delta H_a (\pm \text{S.D})$	$c (\pm \text{S.D})$	$\Delta H_a (\pm \text{S.D})$	$c (\pm \text{S.D})$
		kJ.mol ⁻¹		kJ.mol ⁻¹		kJ.mol ⁻¹		kJ.mol ⁻¹	
<i>Nicotiana tabacum</i>	C ₃	36.4±2.9	15.8±1.2	60.3±1.9	25.5±0.8	37.3±1.4	17.9±0.7	22.5±1.2	-4.7±0.3
<i>Panicum bisulcatum</i>		32.4±8.5	13.9±3.7	71.2±7.2	29.7±3.0	31.0±3.7	15.0±1.8	29.7±2.0	-7.6±0.5
<i>Panicum milioides</i>	C ₂	40.3±0.5	17.0±0.2	68.4±4.2	28.4±1.8	25.4±1.9	12.7±1.0	27.6±3.0	-6.7±0.7
<i>Panicum monticola</i>		30.6±1.8	14.0±0.8	56.5±4.2	24.5±1.8	33.8±1.9	16.9±0.9	n.m	
<i>Cenchrus ciliaris</i>	C ₄ (NADP-ME)	26.3±0.7	12.4±0.3	54.9±3.1	23.9±1.3	22.1±2.4	12.4±1.3	20.3±0.5	-4.0±0.1
<i>Setaria viridis</i>		26.3±2.8	12.4±1.3	56.6±2.8	24.6±1.2	21.4±0.1	11.9±0.1	25.3±4.4	-6.0±1.0
	#Boyd et al 2015	75.0±1.1	31.9±0.5	94.2±10.4	39.3±9.4	44.7±3.8	22.3±1.9	25.2±5.7	-6.2±1.4
<i>Panicum virgatum</i>		31.1±2.9	13.7±1.3	58.1±0.8	24.7±0.3	34.0±4.5	16.9±2.2	23.8±1.9	-5.2±0.4
<i>Panicum milliaceum</i>	C ₄ (NAD-ME)	28.6±4.0	12.3±1.7	71.6±1.8	29.6±0.7	34.9±5.8	16.6±2.7	28.6±6.1	-7.2±1.5
<i>Panicum coloratum</i>		23.2±4.5	10.6±2.1	58.3±4.6	24.8±1.9	21.3±2.8	11.4±1.5	23.5±2.3	-5.1±0.5
<i>Megathyrsus maximus</i>		24.5±1.2	11.6±0.5	50.2±3.3	21.9±1.4	22.2±3.0	12.3±1.7	22.2±3.3	-4.6±0.7
<i>Urochloa panicoides</i>	C ₄ (PCK)	26.9±0.9	12.6±0.4	57.3±4.5	24.8±1.9	29.9±3.0	15.2±1.5	22.3±2.0	-4.6±0.4
<i>Panicum deustum</i>		27.8±1.7	12.8±0.8	59.5±1.3	25.6±0.5	28.7±1.7	14.9±0.9	20.8±2.3	-3.9±0.4
Averages	C ₃ /C ₂	36.3 b	15.5 b	69.8 b	29.0 b	28.2 a	13.9 a	28.6 b	-7.1 a
	NAD-ME	27.6 ab	12.2 a	62.7 ab	26.6 ab	30.0 a	15.0 a	25.3 ab	-5.8 ab
	NADP-ME	27.7 a	12.9 a	56.0 a	24.4 a	25.8 a	13.7 a	22.8 a	-5.0 b
	PCK	26.4 a	12.3 a	55.6 a	24.1 a	26.9 a	14.1 a	21.7 a	-4.4 b
Type (p)		ns(0.081)	ns(0.10)	*	ns(0.062)	ns	ns	ns(0.072)	ns(0.089)

744 Values of ΔH_a and c were determined from measures of k_{cat}^c (Fig S1), $K_C^{21\% \text{ O}_2}$ (Fig S2) and $S_{C/O}$ (Fig S4) made at 10, 15, 20, 25, 30 and 35 (or
745 37)°C (see Table S2 for data) and fitted to the Arrhenius-type equation

$$746 \text{ Parameter} = \exp \left[c - \frac{\Delta H_a}{RT} \right]$$

747 where R the molar gas constant (8.314 J K⁻¹ mol⁻¹) and T the assay temperature (K). n.m, not measured. For each species data are the mean ± SE
748 of at least N=3 biological samples assayed in duplicate. One-way ANOVA was undertaken using the photosynthetic type/subtype as the main
749 factor. Symbols show the statistical significance levels (ns = $p > 0.05$; * = $p < 0.05$), while letters show the ranking of the means using a post hoc

750 Tukey test (different letters indicate statistical differences at the 5% level, $p < 0.05$). # Comparative data for *S. viridis* Rubisco from Boyd et
751 al., (2015)¹⁵ measured by MIMS.

Table S4. Summary of parameters used in the modelling plots shown in Figure 4 and Figure S5.

Species	Parameters	Temperature (°C)						Reference
		10	15	20	25	30	37	
<i>Nicotiana tabacum</i>	k_{cat}^c (s ⁻¹)	1.4	1.8	2.4	3.1	4.7	8.0	Tables S1-2
	$K_{C^{air}}$ (μM)	7.9	10.4	13.6	17.6	22.5	31.4	Tables S1-2
	$S_{C/O}$ (M M ⁻¹)	131	111	95	81	70	57	Tables S1-2
	J_{max}/V_{cmax}	2.6	2.1	1.8	1.6	1.4	1.2	Sharkey <i>et al.</i> (2007) ²⁷
<i>Panicum bisulcatum</i>	k_{cat}^c (s ⁻¹)	1.2	1.6	2.0	2.6	4.2	8.0	Tables S1-2
	$K_{C^{air}}$ (μM)	6.2	7.8	9.7	12.1	14.8	19.6	Tables S1-2
	$S_{C/O}$ (M M ⁻¹)	156	125	101	83	68	52	Tables S1-2
<i>Panicum deustum</i>	k_{cat}^c (s ⁻¹)	2.7	3.3	4.1	5.1	7.6	12.9	Tables S1-2
	$K_{C^{air}}$ (μM)	14.6	18.1	22.2	27.1	32.8	42.4	Tables S1-2
	$S_{C/O}$ (M M ⁻¹)	132	114	98	85	74	61	Tables S1-2
<i>Urochloa panicoides</i>	k_{cat}^c (s ⁻¹)	3.2	3.8	4.7	5.6	8.3	13.9	Tables S1-2
	$K_{C^{air}}$ (μM)	12.5	15.5	19.2	23.6	28.8	37.6	Tables S1-2
	$S_{C/O}$ (M M ⁻¹)	125	106	91	78	67	55	Tables S1-2
Common parameters	g_m (mol m ⁻² s ⁻¹ bar ⁻¹)	0.24	0.33	0.44	0.57	0.72	0.97	von Caemmerer and Evans (2015) ⁴⁹
	TPU (μmol m ⁻² s ⁻¹)	3.81	5.62	8.14	11.40	14.65	14.10	Sharkey <i>et al.</i> (2007) ²⁷
	R_d (μmol m ⁻² s ⁻¹)	0.37	0.52	0.73	1.04	1.36	2.06	Sharkey <i>et al.</i> (2007) ²⁷
	s_c (M bar ⁻¹)	0.0512	0.0442	0.0383	0.0334	0.0292	0.0245	https://en.wikipedia.org/wiki/Henry's_law
	s_o (M bar ⁻¹)	0.00170	0.00154	0.00139	0.00126	0.00115	0.00101	https://en.wikipedia.org/wiki/Henry's_law
	J_{max} (μmol m ⁻² s ⁻¹)	63	87	118	160	214	317	Sharkey <i>et al.</i> (2007) ²⁷
	Rubisco sites (μmol s ⁻¹)	30	30	30	30	30	30	

753 Photosynthesis rate, A was calculated as $A = \min(A_c, A_j, A_t)$, where A_c , A_j and A_t are the CO₂-limited (A_c), light-limited (A_j) and the triose
754 phosphate utilisation (TPU)-limited (A_t) assimilation rates, respectively. Their expressions are defined as:

755
$$A_c = \frac{m \cdot k_{cat}^c (C_c \cdot S_c - 0.5 O_c / S_{C/O})}{(C_c \cdot S_c + K_{C^{air}})} - R_d ;$$

756 $A_j = \frac{(C_c \cdot S_c - 0.5 O_c / S_{c/o}) J_{\max}}{4(C_c \cdot S_c + O_c / S_{c/o})} - R_d$; and

757 $A_t = 3TPU - R_d$.

758 The model parameters used are: m = amount of leaf Rubisco set at 30 μmol active sites m^{-2} ; k_{cat}^c (s^{-1}) = Rubisco carboxylation rate; K_C^{air}
 759 (μM) = Michaelis-Menten constant of Rubisco for CO_2 and $S_{c/o} = \text{CO}_2/\text{O}_2$ specificity of Rubisco. The maximal RuBP carboxylation-
 760 limited assimilation rate, $V_{\text{cmax}} = m \cdot k_{\text{cat}}^c$. The maximal RuBP regeneration-limited assimilation rate, J_{\max} ($\mu\text{mol m}^{-2} \text{s}^{-1}$) is set to equal
 761 $1.7V_{\text{cmax}}$ for tobacco at 25°C ; its values at other temperatures were calculated using the thermal dependence from Bernacchi et al (2003)
 762 ⁵⁰:

763 $J_{\max}(T) = J_{\max_{25}} \cdot e^{\left(c - \frac{Ha}{R \cdot (273+T)}\right)}$, where $c = 17.7$ and $\Delta H_a = 43.9$ (in kJ mol^{-1}).

764 The values at 25°C for TPU ($11.4 \mu\text{mol m}^{-2} \text{s}^{-1}$) and mitochondrial respiration, R_d ($1 \mu\text{mol m}^{-2} \text{s}^{-1}$) and their thermal dependence were
 765 adapted from Sharkey et al (2007) ²⁷:

766 $R_d(T) = R_{d_{25}} \cdot e^{\left(c - \frac{Ha}{R \cdot (273+T)}\right)}$, where $c = 18.72$ and $\Delta H_a = 46.4$ (in kJ mol^{-1})

767 $TPU(T) = TPU_{25} \left[\frac{e^{\left(c - \frac{Ha}{R \cdot (273+T)}\right)}}{1 + e^{\left(\frac{S \cdot (273+T) \cdot Hd}{R \cdot (273+T)}\right)}} \right]$, where $c = 21.46$ and $\Delta H_a = 53.1$, $\Delta H_d = 201.8$ and 0.65 (in kJ mol^{-1}).

768 C_c and O_c are the CO₂ and O₂ concentrations in the chloroplast, respectively. Gas concentrations in the liquid phase were calculated
769 using the solubility constants for CO₂ ($s_c = 0.0334 \text{ M bar}^{-1}$) and O₂ ($s_o = 0.00126 \text{ M bar}^{-1}$) at 25°C. Their thermal dependence was
770 determined according to Henry's law using the following expressions (https://en.wikipedia.org/wiki/Henrys_law):

771 $s_c(T) = s_{c_{25}} \cdot 2400 \cdot e^{\left(\frac{1}{273+T} - \frac{1}{298}\right)}$ and

772 $s_o(T) = s_{o_{25}} \cdot 1700 \cdot e^{\left(\frac{1}{273+T} - \frac{1}{298}\right)}$

773 Intercellular CO₂ concentration, C_i was calculated using a constant C_i/C_a ratio of 0.70⁴⁹. C_c was calculated as $C_c = C_i - A/g_m$, where g_m
774 is the mesophyll conductance to CO₂ transfer. Tobacco g_m at 25°C ($0.57 \text{ mol m}^{-2} \text{ s}^{-1} \text{ bar}^{-1}$) and its thermal dependence were taken from
775 von Caemmerer and Evans (2015)⁴⁹.

776 **Table S5. Parameters used to calculate CO₂ concentrations in ¹⁴CO₂-fixation**
 777 **assays at the varying temperatures.**

Parameter (<i>units</i>)	Value					
	(10°C)	(15°C)	(20°C)	(25°C)	(30°C)	(37°C)
<i>T</i> ; assay temperature	283K	288K	293K	298K	303K	310K
<i>q</i> ; CO ₂ solubility at 1 atm (<i>Mol.L⁻¹.atm⁻¹</i>)	0.0524	0.0455	0.0382	0.0329	0.0289	0.0240
<i>R</i> : universal gas constant (<i>L.atm.K⁻¹.mol⁻¹</i>)	0.082057					
pK ₁	6.362	6.327	6.280	6.251	6.226	6.202
pK ₂	10.499	10.431	10.377	10.329	10.290	10.238
*pH	8.27	8.24	8.21	8.16	8.11	8.03

778 The values were fitted to the Henderson-Hasselbalch derived equation

779
$$[CO_2] = \frac{(C_t)}{1 + \frac{V}{vqRT} + 10^{(pH-pK_1)} + 10^{(2pH-pK_1-pK_2)}}$$

780 *V/v*: ratio of reaction vial headspace (*V*) to assay volume (*v*).

781 *example pH variation for 50 mM EPPES-NaOH buffer adjusted to pH 8.16 at 25°C; the

782 0.26 pH variation has <1% effect on tobacco Rubisco carboxylase activity.

783 **References**

- 784 1 Andrews, T. J. & Whitney, S. M. Manipulating ribulose biphosphate
 785 carboxylase/oxygenase in the chloroplasts of higher plants. *Arch.Biochem.Biophys.*
 786 **414**, 159-169 (2003).
- 787 2 Carmo-Silva, E., Scales, J. C., Madgwick, P. J. & Parry, M. A. J. Optimizing
 788 Rubisco and its regulation for greater resource use efficiency. *Plant Cell Env* **38**,
 789 1817-1832 (2015).
- 790 3 Raven, J. A. Rubisco: still the most abundant protein of Earth? *New Phytol* **198**, 1-
 791 3 (2013).
- 792 4 Sage, R. F. The evolution of C₄ photosynthesis *New Phytol* **161**, 341-370 (2004).
- 793 5 Sage, R. F., Christin, P.-A. & Edwards, E. J. The C₄ plant lineages of planet Earth.
 794 *J Exp Bot* **62**, 3155-3169 (2011).
- 795 6 Furbank, R. T. Evolution of the C₄ photosynthetic mechanism: are there really three
 796 C₄ acid decarboxylation types? *J Exp Bot* **62**, 3103-3108 (2011).
- 797 7 Sage, R. F., Sage, T. L. & Kocacinar, F. Photorespiration and the evolution of C₄
 798 photosynthesis. *Ann Rev Plant Biol* **63**, 19-47 (2012).
- 799 8 Sharwood, R. E., Ghannoum, O. & Whitney, S. M. Prospects for improving CO₂
 800 fixation in C₃-crops through understanding C₄-Rubisco biogenesis and catalytic
 801 diversity. *Curr Opin Plant Biol* **31**, 135-142 (2016).
- 802 9 Ghannoum, O. *et al.* Faster rubisco is the key to superior nitrogen-use efficiency in
 803 NADP-malic enzyme relative to NAD-malic enzyme C₄ grasses. *Plant Physiol* **137**,
 804 638-650 (2005).
- 805 10 von Caemmerer, S., Quick, W. P. & Furbank, R. T. The development of C₄ rice:
 806 current progress and future challenges. *Science* **336**, 1671-1672 (2012).
- 807 11 Sharwood, R., von Caemmerer, S., Maliga, P. & Whitney, S. The catalytic
 808 properties of hybrid Rubisco comprising tobacco small and sunflower large
 809 subunits mirror the kinetically equivalent source Rubiscos and can support tobacco
 810 growth. *Plant Physiol* **146**, 83-96 (2008).
- 811 12 Sharwood, R. E., Sonawane, B. V., Ghannoum, O. & Whitney, S. M. Improved
 812 analysis of C₄ and C₃ photosynthesis via refined in vitro assays of their carbon
 813 fixation biochemistry. *J Exp Bot* **67**, 3137-3148 (2016).
- 814 13 Whitney, S. M. & Sharwood, R. E. Construction of a tobacco master line to improve
 815 Rubisco engineering in chloroplasts. *J Exp Bot* **59**, 1909-1921 (2008).
- 816 14 Tcherkez, G. G. B., Farquhar, G. D. & Andrews, T. J. Despite slow catalysis and
 817 confused substrate specificity, all ribulose biphosphate carboxylases may be
 818 nearly perfectly optimized. *Proc Nat Acad Sci* **103**, 7246-7251 (2006).
- 819 15 Boyd, R. A., Gandin, A. & Cousins, A. B. Temperature response of C₄
 820 photosynthesis: biochemical analysis of Rubisco, phosphoenolpyruvate
 821 carboxylase and carbonic anhydrase in *Setaria viridis*. *Plant Physiol* **169**, 1850-
 822 1861 (2015).
- 823 16 Carmo-Silva, A. E. *et al.* Rubisco activities, properties, and regulation in three
 824 different C₄ grasses under drought. *J Exp Bot* **61**, 2355-2366 (2010).
- 825 17 Galmes, J. *et al.* Expanding knowledge of the Rubisco kinetics variability in plant
 826 species: environmental and evolutionary trends. *Plant Cell Environ* **37**, 1989-2001
 827 (2014).

- 828 18 Galmés, J., Kapralov, M. V., Copolovici, L. O., Hermida-Carrera, C. & Niinemets,
829 Ü. Temperature responses of the Rubisco maximum carboxylase activity across
830 domains of life: phylogenetic signals, trade-offs, and importance for carbon gain.
831 *Photosynth Res* **123**, 183-201 (2015).
- 832 19 Perdomo, J. A., Cavanagh, A. P., Kubien, D. S. & Galmés, J. Temperature
833 dependence of in vitro Rubisco kinetics in species of *Flaveria* with different
834 photosynthetic mechanisms. *Photosynth Res* **124**, 67-75 (2015).
- 835 20 Sage, R. F. Variation in the k_{cat} of Rubisco in C₃ and C₄ plants and some
836 implications for photosynthetic performance at high and low temperature. *J Exp*
837 *Bot* **53**, 609-620 (2002).
- 838 21 Savir, Y., Noor, E., Milo, R. & Tlusty, T. Cross-species analysis traces adaptation
839 of Rubisco toward optimality in a low-dimensional landscape. *Proc Nat Acad Sci*
840 **107**, 3475-3480 (2010).
- 841 22 Percy, R. W. & Ehleringer, J. Comparative ecophysiology of C₃ and C₄ plants.
842 *Plant Cell Env* **7**, 1-13 (1984).
- 843 23 Tcherkez, G. The mechanism of Rubisco-catalyzed oxygenation. *Plant Cell Env*
844 **39**, 983-997 (2016).
- 845 24 Farquhar, G. D., von Caemmerer, S. & Berry, J. A. A biochemical model of
846 photosynthetic CO₂ assimilation in leaves of C₃ species. *Planta* **149**, 78-90 (1980).
- 847 25 Sharwood, R. E. & Whitney, S. M. Correlating Rubisco catalytic and sequence
848 diversity within C₃ plants with changes in atmospheric CO₂ concentrations. *Plant*
849 *Cell Env* **37**, 1981-1984 (2014).
- 850 26 Young, J. N. *et al.* Large variation in the Rubisco kinetics of diatoms reveals
851 diversity among their carbon-concentrating mechanisms. *J Exp Bot* **67**, 3445-3456
852 (2016).
- 853 27 Sharkey, T. D., Bernacchi, C. J., Farquhar, G. D. & Singaas, E. L. Fitting
854 photosynthetic carbon dioxide response curves for C₃ leaves. *Plant Cell Env* **30**,
855 1035-1040 (2007).
- 856 28 Walker, B., Ariza, L. S., Kaines, S., Badger, M. R. & Cousins, A. B. Temperature
857 response of *in vivo* Rubisco kinetics and mesophyll conductance in *Arabidopsis*
858 *thaliana*: comparisons to *Nicotiana tabacum*. *Plant Cell Env* **36**, 2108-2119 (2013).
- 859 29 Whitney, S. M., Houtz, R. L. & Alonso, H. Advancing our understanding and
860 capacity to engineer nature's CO₂-sequestering enzyme, Rubisco. *Plant Physiol*
861 **155**, 27-35 (2011).
- 862 30 Hermida-Carrera, C., Kapralov, M. V. & Galmés, J. Rubisco catalytic properties
863 and temperature response in crops. *Plant Physiol.*, doi:10.1104/pp.16.01846
864 (2016).
- 865 31 Orr, D. *et al.* Surveying Rubisco diversity and temperature response to improve
866 crop photosynthetic efficiency. *Plant Physiol.*, doi:10.1104/pp.16.00750 (2016).
- 867 32 Badger, M. R. & Collatz, G. J. Studies on the kinetic mechanism of RuBP
868 carboxylase and oxygenase reactions, with particular reference to the effect of
869 temperature on kinetic parameters. *Carnegie YB* **76**, 355-361 (1977).
- 870 33 Jordan, D. B. & Ogren, W. L. The CO₂/O₂ specificity of ribulose 1,5-bisphosphate
871 carboxylase oxygenase - dependence on ribulosebisphosphate concentration, pH
872 and temperature. **161**, 308-313 (1984).

- 873 34 Ishikawa, C., Hatanaka, T., Misoo, S., Miyake, C. & Fukayama, H. Functional
874 incorporation of sorghum small subunit increases the catalytic turnover rate of
875 Rubisco in transgenic rice *Plant Physiol* **156**, 1603-1611 (2011).
- 876 35 Prins, A. *et al.* Rubisco catalytic properties of wild and domesticated relatives
877 provide scope for improving wheat photosynthesis. *J Exp Bot* **67**, 1827-1838
878 (2016).
- 879 36 Hauser, T., Popilka, L., Hartl, F. U. & Hayer-Hartl, M. Role of auxiliary proteins
880 in Rubisco biogenesis and function. *Nat Plants* **1** (2015).
- 881 37 Wachter, R. M. *et al.* Activation of interspecies-hybrid Rubisco enzymes to assess
882 different models for the Rubisco-Rubisco activase interaction. *Photosynth Res* **117**,
883 557-566 (2013).
- 884 38 Andersson, I. & Backlund, A. Structure and function of Rubisco. *Plant Physiol*
885 *Biochem* **46**, 275-291 (2008).
- 886 39 Spreitzer, R. J., Peddi, S. R. & Satagopan, S. Phylogenetic engineering at an
887 interface between large and small subunits imparts land-plant kinetic properties to
888 algal Rubisco. *Proc Natl Acad Sci* **102**, 17225-17230 (2005).
- 889 40 Andersson, I. Catalysis and regulation in Rubisco. *J Exp Bot* **59**, 1555-1568 (2008).
- 890 41 von Caemmerer, S. & Furbank, R. T. The C₄ pathway: an efficient CO₂ pump.
891 *Photosynth Res* **77**, 191-207, doi:10.1023/a:1025830019591 (2003).
- 892 42 Still, C. J., Pau, S. & Edwards, E. J. Land surface skin temperature captures thermal
893 environments of C₃ and C₄ grasses. *Glob Ecol Biogeo* **23**, 286-296 (2014).
- 894 43 Galmés, J. *et al.* Environmentally driven evolution of Rubisco and improved
895 photosynthesis and growth within the C₃ genus *Limonium* (Plumbaginaceae). *New*
896 *Phytol* **203**, 989-999 (2014).
- 897 44 Whitney, S. M. & Andrews, T. J. Plastome-encoded bacterial ribulose-1, 5-
898 bisphosphate carboxylase/oxygenase (RubisCO) supports photosynthesis and
899 growth in tobacco. *Proc Nat Acad Sci* **98**, 14738-14743 (2001).
- 900 45 Parry, M. A. J. *et al.* Rubisco activity and regulation as targets for crop
901 improvement. *J Exp Bot* **64**, 717-730 (2013).
- 902 46 Bortesi, L. & Fischer, R. The CRISPR/Cas9 system for plant genome editing and
903 beyond. *Biotech Adv* **33**, 41-52 (2015).
- 904 47 Stamatakis, A. RAxML version 8: a tool for phylogenetic analysis and post-
905 analysis of large phylogenies. *Bioinform* **30**, 1312-1313 (2014).
- 906 48 Whitney, S. M., Birch, R., Kelso, C., Beck, J. L. & Kapralov, M. V. Improving
907 recombinant Rubisco biogenesis, plant photosynthesis and growth by coexpressing
908 its ancillary RAF1 chaperone. *Proc Natl Acad Sci* **112**, 3564-3569 (2015).
- 909 49 von Caemmerer, S. & Evans, J. R. Temperature responses of mesophyll
910 conductance differ greatly between species. *Plant Cell Env* **38**, 629-637 (2015).
- 911 50 Bernacchi, C. J., Pimentel, C. & Long, S. P. In vivo temperature response functions
912 of parameters required to model RuBP-limited photosynthesis. *Plant Cell Env* **26**,
913 1419-1430 (2003).

914

915